60 K PHASE CHANGE MATERIAL DEVICE

David C. Bugby

Swales & Associates, Inc.
5050 Powder Mill Road
Beltsville, MD 20705

January 1996

Final Report

PHILLIPS LABORATORY
Space Technology Directorate
AIR FORCE MATERIEL COMMAND
KIRTLAND AIR FORCE BASE, NM 87117-5776

AD NUMBER

AD-B215 545

NEW LIMITATION CHANGE

TO

DISTRIBUTION STATEMENT A -
Approved for public release; Distribution unlimited.

Limitation Code: 1

FROM

DISTRIBUTION STATEMENT -

Limitation Code:

AUTHORITY

Janet E. Mosher; Phillips Lab/CA, Kirtland AFB, N.M.

PL-TR-96-1026

This report has been approved for publication.

Michael R. Rich

MICHAEL R. RICH, Lt, USAF
Project Manager

FOR THE COMMANDER

Paul L. Thee

PAUL L. THEE, Maj, USAF
Chief, Space Power & Thermal
Management Division

Christine M. Anderson

CHRISTINE M. ANDERSON
Director, Space and Missiles Technology
Directorate

The following notice applies to any unclassified (including originally classified and now declassified) technical reports released to "qualified U.S. contractors" under the provisions of DoD Directive 5230.25, Withholding of Unclassified Technical Data From Public Disclosure.

NOTICE TO ACCOMPANY THE DISSEMINATION OF EXPORT-CONTROLLED TECHNICAL DATA

1. Export of information contained herein, which includes, in some circumstances, release to foreign nationals within the United States, without first obtaining approval or license from the Department of State for items controlled by the International Traffic in Arms Regulations (ITAR), or the Department of Commerce for items controlled by the Export Administration Regulations (EAR), may constitute a violation of law.

2. Under 22 U.S.C. 2778 the penalty for unlawful export of items or information controlled under the ITAR is up to two years imprisonment, or a fine of $100,000, or both. Under 50 U.S.C., Appendix 2410, the penalty for unlawful export of items or information controlled under the EAR is a fine of up to $1,000,000, or five times the value of the exports, whichever is greater; or for an individual, imprisonment of up to 10 years, or a fine of up to $250,000, or both.

3. In accordance with your certification that establishes you as a "qualified U.S. Contractor", unauthorized dissemination of this information is prohibited and may result in disqualification as a qualified U.S. contractor, and may be considered in determining your eligibility for future contracts with the Department of Defense.

4. The U.S. Government assumes no liability for direct patent infringement, or contributory patent infringement or misuse of technical data.

5. The U.S. Government does not warrant the adequacy, accuracy, currency, or completeness of the technical data.

6. The U.S. Government assumes no liability for loss, damage, or injury resulting from manufacture or use for any purpose of any product, article, system, or material involving reliance upon any or all technical data furnished in response to the request for technical data.

7. If the technical data furnished by the Government will be used for commercial manufacturing or other profit potential, a license for such use may be necessary. Any payments made in support of the request for data do not include or involve any license rights.

8. A copy of this notice shall be provided with any partial or complete reproduction of these data that are provided to qualified U.S. contractors.

DESTRUCTION NOTICE

For classified documents, follow the procedures in DoD 5200.22-M, Industrial Security Manual, Section II-19 or DoD 5200.1-R, Information Security Program Regulation, Chapter IX. For unclassified, limited documents, destroy by any method that will prevent disclosure of contents or reconstruction of the document.

DRAFT SF 298

1. Report Date (dd-mm-yy)	2. Report Type	3. Dates covered (from... to)
January 1996	Final	04/94 to 04/95

4. Title & subtitle
60 K Phase Change Material Device

5a. Contract or Grant # F29601-94-C-0099

5b. Program Element # 62601F

6. Author(s)
David C. Bugby

5c. Project # 3005

5d. Task # C0

5e. Work Unit # FR

7. Performing Organization Name & Address
Swales & Associates, Inc.
5050 Powder Mill Road
Beltsville, MD 20705

8. Performing Organization Report #
SAI-RPT-051

9. Sponsoring/Monitoring Agency Name & Address
Phillips Laboratory
3550 Aberdeen Ave SE
Kirtland AFB, NM 87117-5776

10. Monitor Acronym

11. Monitor Report #
PL-TR-96-1026

12. Distribution/Availability Statement
Distribution authorized to DoD and U.S. DoD contractors only; Critical Technology; January 1996. Other requests shall be referred to AFMC/STI.

13. Supplementary Notes

14. Abstract The objective of this Phase I SBIR program was to demonstrate the feasibility of phase change material device (PCMD) technology at 60 K. The application for this technology will be to optimize the performance, improve the reliability, and reduce the cost of space-based infrared (IR) sensor systems for the DoD. In Phase I, an apparatus was designed and constructed for testing/characterizing PCMs and PCMDs, a one-tenth scale prototype PCMD was designed, analyzed, fabricated, and successfully tested, and four PCMs - nitrogen, freon-22, air, and nitrogen trifluoride - were performance tested. In addition, a plan was prepared for continued Phase II development. The experimental results indicate that nitrogen trifluoride is a very promising 60 K PCM. In particular, the testing showed that a nitrogen trifluoride-based PCMD has over two times the energy storage capacity of a nitrogen-based PCMD, and four times the energy storage capacity of a high heat capacity solid device.

15. Subject Terms Phase Change, Thermal Storage, Cryogenics, IR Sensors, Thermal Load Levelling

Security Classification of			19. Limitation of Abstract	20. # of Pages	21. Responsible Person (Name and Telephone #)
16. Report Unclassified	17. Abstract Unclassified	18. This Page Unclassified	Limited	56	Lt Michael Rich (505) 846-0443

TABLE OF CONTENTS

LIST OF FIGURES

LIST OF TABLES

SUMMARY

This report summarizes the work performed on the 60 K Phase Change Material Device program, which was a Phase I SBIR sponsored by Phillips Laboratory. The principal objective of the Phase I program was to demonstrate the feasibility of phase change material device (PCMD) technology at 60 K. The application for this technology is to optimize the performance, improve the reliability, and reduce the cost of space-based infrared (IR) sensor systems for the DoD. In Phase I, an apparatus was designed and constructed for testing/characterizing PCMs and PCMDs, a one-tenth scale prototype PCMD was designed, analyzed, fabricated, and successfully tested, and four PCMs -- nitrogen, freon-22, air, and nitrogen trifluoride -- were performance tested. In addition, a plan was prepared for continued Phase II development. The experimental results indicate that nitrogen trifluoride is a very promising 60 K PCM. In particular, the testing showed that a nitrogen trifluoride-based PCMD has over two times the energy storage capacity of a nitrogen-based PCMD, and four times the energy storage capacity of a high heat capacity solid device (Mg-Li alloy with ΔT=1K, PCMD with NF_3-to-solid ratio of 15%). As a direct result of this effort, it can be definitively stated that constructing a PCMD for use at 60 K is feasible. The objective, approach, results, future plans, and commercial applications for 60 PCMD technology are summarized in detail in this report.

1.0 Introduction

Mechanically cooled, long-life IR sensor systems for the DoD require a constant operating temperature (60 K in the application of interest here) and a vibration-free environment for optimum performance. However, cryocoolers induce vibration, consume electrical power, and have demonstrated only moderate lifetimes. In these DoD systems, it would be advantageous to be able to occasionally and temporarily turn off the cryocooler to provide temporary periods of vibration-free operation, reduce the average electrical power consumption, and level thermal loads. To maintain a constant focal plane temperature while the cryocooler is disabled, a device is needed to isothermally store the heat generated by the sensor hardware. The "thermal storage unit" or TSU would also smooth out heating transients during cryocooler operation, thus the cryocooler could be sized for the average rather than the peak heating load. The benefits of a properly designed TSU are improved IR sensor system performance, reduced power consumption, and lower system cost. Figure 1 illustrates a possible application for thermal storage device technology in a mechanically-cooled IR sensor system.

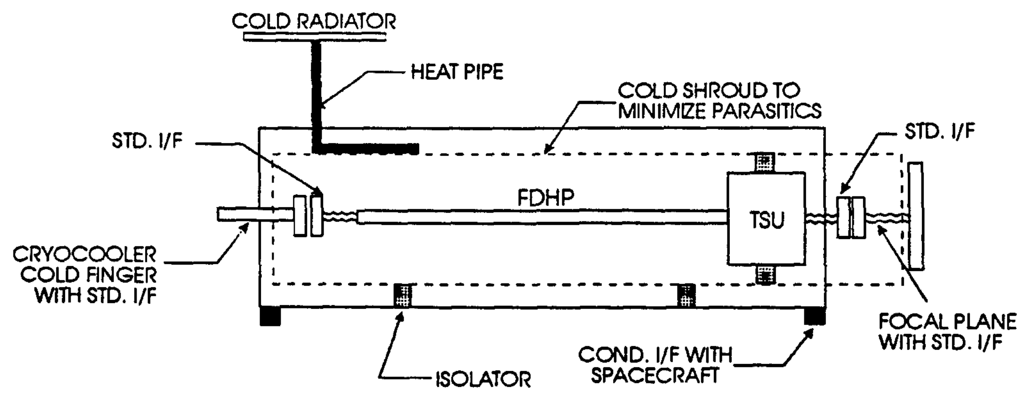

Figure 1. Application for Thermal Storage Device in IR Sensor System

In the application pictured above, the TSU incorporates a material (or material mixture) that isothermally absorbs energy at or near 60 K. To obtain isothermal operation, the energy storage material must undergo a sufficiently energetic phase transition such as melting (solid-to-liquid), vaporization (liquid-to-gas), sublimation (solid-to-gas), or crystal structure realignment (solid-to-solid). Preliminary trade studies indicate that phase transitions that occur with small changes in density (e.g., melting or crystal structure realignment) will require the least volume and weight to implement. However, at present, there is very little experimental data on energy storage device performance at temperatures near 60 K. The ideal phase change material (PCM) is one that has a transition temperature near 60 K, is chemically stable, has a high heat of transition, is safe to use, exhibits no supercooling behavior, has a small density change on transition, and is compatible with common metal containers. The ideal container for the PCM is one that interfaces easily with the sensor hardware, provides containment at room temperature, maximizes the transport of energy to (and away from) the phase change material, and minimizes the internal thermal gradients.

With the foregoing in mind, the principal objective of this Phase I SBIR program was to demonstrate the feasibility of developing a 60 K phase change material device

(PCMD) to be incorporated into the overall TSU. This report outlines the progress made toward that end and is organized as follows. In Section 2.0, the problem background is outlined including the technical requirements, an overview of the technical approach, and a brief description of the concept used for developing the PCMD prototype. In Section 3.0, the Phase I technical approach is described, including a review of PCM technology, a description of the test apparatus, a detailed description of the prototype PCMD, and a summary of the analytical modeling. In Section 4.0, the experimental procedure, results, and analysis of the results are provided. In Sections 5.0 and 6.0, the plan for continued Phase II development is presented. Included in this plan is a detailed discussion of potential commercial PCMD applications.

2.0 Program Background

2.1 Technical Requirements

The technical requirements for the 60 K Thermal Storage Unit (TSU), as outlined at the beginning of Phase I, are listed below. The Phase I development program was structured so that the technical requirements could be easily achieved during Phase II.

• Temperature	60-65 K
• Temperature Stability	+/- 0.5 K
• Cycle Time Period	100 min
• Baseline Heat Loads	5.0 W (operating), 1.0 W (non-operating)
• Peak Load Duty Cycle	50 %
• Minimum Energy Storage	6000 J
• Maximum Weight	3.5 kg
• Maximum Volume	1500 cc

2.2 Overview of Approach

To be able to meet the above requirements during Phase II, the Phase I development program was comprised of the following elements: (1) conduct a thorough review of the available scientific and engineering literature for information on low temperature PCMs and PCMDs; (2) design and assemble a test apparatus for testing prototype and flight PCMDs at 60 K; (3) design, analyze, and fabricate a one-tenth scale prototype PCMD to characterize candidate PCMs; (4) design, analyze, and calibrate a Q-meter for measuring the heat flow between the cryocooler and the PCMD; (5) conduct tests to characterize four potential PCM fluids (nitrogen, freon-22, nitrogen trifluoride, and nitrogen/argon mixtures) at or near 60 K; and (6) extend the design of the one-tenth scale PCMD prototype to meet flight requirements.

2.3 Concept for PCMD Prototype

A concept was developed for a prototype PCMD that could be used to characterize the performance of candidate PCMs. The concept had three primary features: (1) the PCMD outer shell would be a pressure vessel so that any PCM, even those with low critical temperatures and pressures, could be safely tested; (2) the PCMD outer shell and inner core would be made from a solid block of high thermal conductivity

material (2219 Aluminum) to ensure the entire device would be isothermal under any reasonable heat load; and (3) the core would be formed by drilling a large number of parallel, small diameter holes. In normal operation, the PCM would condense within the core region, and the principal resistance in the system would be within the PCM itself. The basic thermal design problem was to size the holes to reduce the intra-PCM temperature gradient to an acceptably low value. The advantages of this design are its conceptually simple operation and ease of manufacture. A simplified thermal network representation of this PCMD concept is provided in Figure 2.

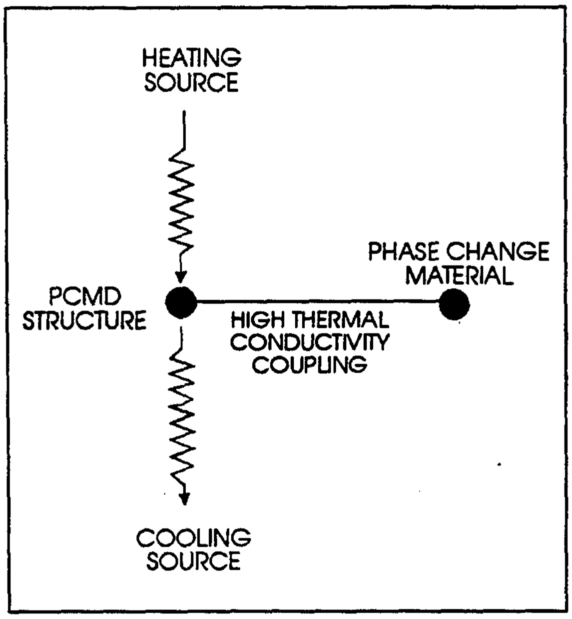

Figure 2. Simplified Thermal Network Representation of PCMD Concept

3.0 Technical Approach

3.1 Review of PCM Technology

The first step was to review a detailed report by Energy Sciences Laboratories, Inc. on cryogenic PCMs [1]. Next, a thorough review of the holdings at the NASA/GSFC library was conducted. Then, Mainstream Engineering (ME) was contracted to conduct a literature review of low temperature solid-liquid PCMs. The ME final report [2] identified nine compounds that have a solid-liquid transition in the range 50-75K but only one material, molecular nitrogen, with a phase transition in the range 60-65 K. Additionally, PJB Engineering was hired during the first month of Phase I to provide technical review services. The principals from PJB participated in the design and testing of the 120 K PCMD (BETSU) developed by Grumman for Phillips Laboratory. Several documents which describe BETSU design, analysis, and testing [3-8] were also reviewed. As a result of the literature review effort described above, a list of PCMs that have phase transitions in the range 55-65 K was prepared. This compilation, which also indicates key PCM properties, is provided in Table 1.

3.2 Test Apparatus

A novel test apparatus was designed and constructed during Phase I to test prototype and flight PCMDs and characterize 60 K PCMs. The test apparatus is illustrated in Figure 3. The test system consists of the following: (1) a 30 K single-stage G-M cryocooler and controller supplied by R.G. Hansen; (2) a vacuum chamber with four instrumentation feed-throughs; (3) a portable vacuum roughing pump capable of 10^{-3} microns; (4) a liquid nitrogen-cooled shroud with inlet/exit feed throughs on the vacuum chamber top flange; (5) four Lakeshore Cryogenics silicon diode temperature sensors; and (6) an 8-channel Lakeshore silicon diode reader. The silicon diode reader output was connected to a PC running the LABVIEW computer program. With LABVIEW, the

temperature data was automatically recorded at prescribed time intervals during the course of testing. The cooling capability of the cryocooler as a function of temperature is shown in Figure 4.

Table 1. Compilation of Cryogenic PCM Properties

PC Temp (K)	Compound	PC Energy (J/g)	PC Type	MP (K)	BP (K)	Tc (K)	Pc (psi)	Liquid Density (g/cc)	Safety
55	Palladium Hydride		S-S						
55.8	Oxygen/Argon Peritectic		Melt	55.8					
56.7	Nitrogen Trifluoride	21.3	S-S	64.5	144	234	657	1.53 at BP	Toxic if Inhaled
58	Gold Zinc Compound		S-S						
59	Air		Melt	59	78.7				
59	Freon-22		S-S	113	232	369	722	1.06 at 54 C	Toxic if Inhaled
61.8	Carbon Monoxide	22.6	S-S	67.5	81.5	133	508	0.79 at BP	Toxic if Inhaled Flammable
63.2	Nitrogen	25.7	Melt	63.2	77.5	122	493	0.87 at MP	
63.5	Silane	19.2	S-S	88.5	161.8	269	703	0.68 at MP	Spontaneously Flammable in Air
64.5	Nitrogen Trifluoride	5.6	Melt	64.5	144	234	657	1.53 at BP	Toxic if Inhaled

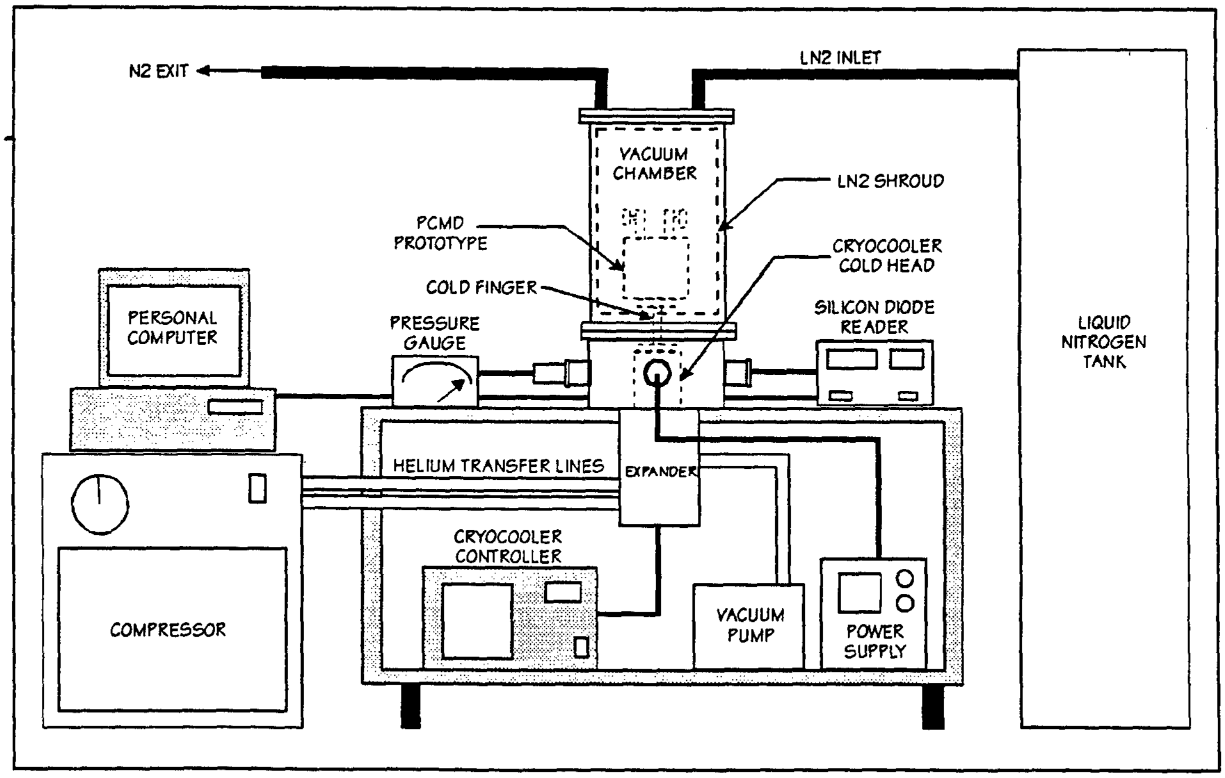

Figure 3. Test Apparatus for 60 K PCMD

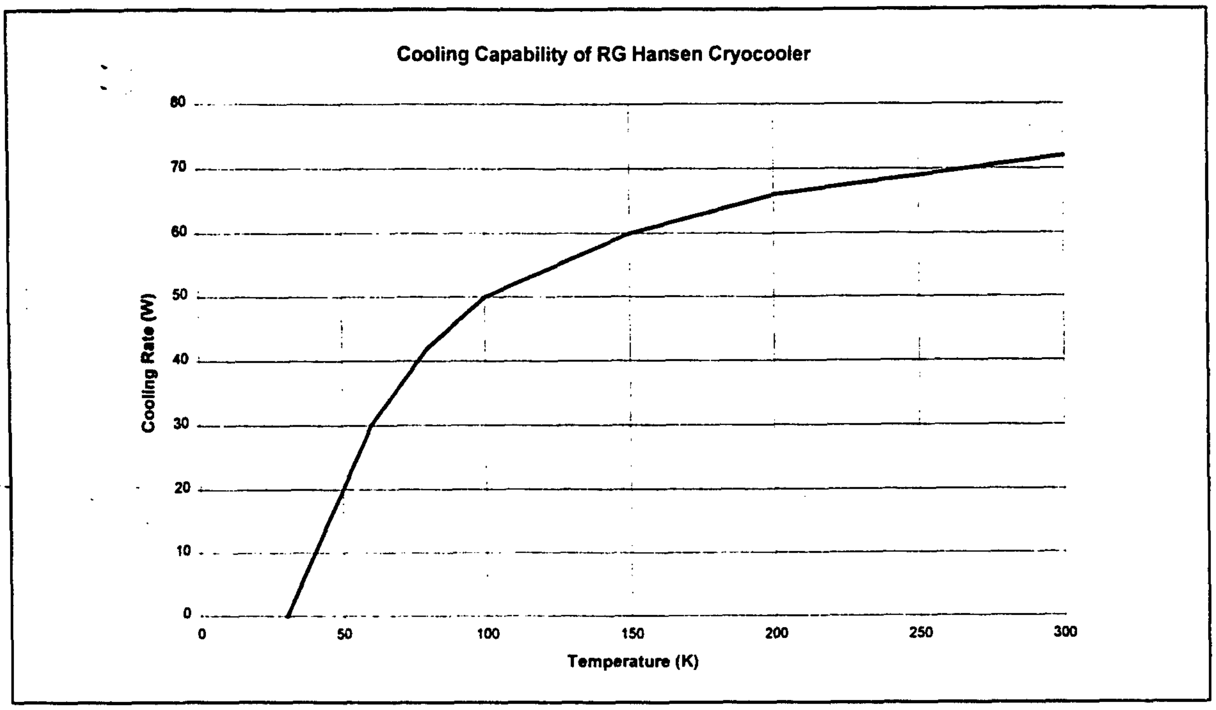

Figure 4. R.G. Hansen Cryocooler Cooling Capability

3.3 PCMD Prototype, Q-Meter, and Heater/Temperature Sensor Placement

The prototype PCMD was designed to provide approximately 600 J of fusion or solid-solid transition phase change energy over the temperature range 60-65 K. The device is a cylindrical, 2219 aluminum pressure vessel with a varying 3-3.5" outer diameter, constant 3.5" length, and varying 0.25-0.5" wall thickness. The device was designed to contain an internal pressure of 3000 psi with a safety factor of 2 (6000 psi design burst pressure). The device has a large internal surface area created by 176 internal 0.125" x 2.25" cylindrical holes which provide a high conductive coupling between the selected working fluid and the aluminum structure. The prototype PCMD was pressure tested to 4500 psi and helium leak tested. Figure 5 illustrates the prototype PCMD design.

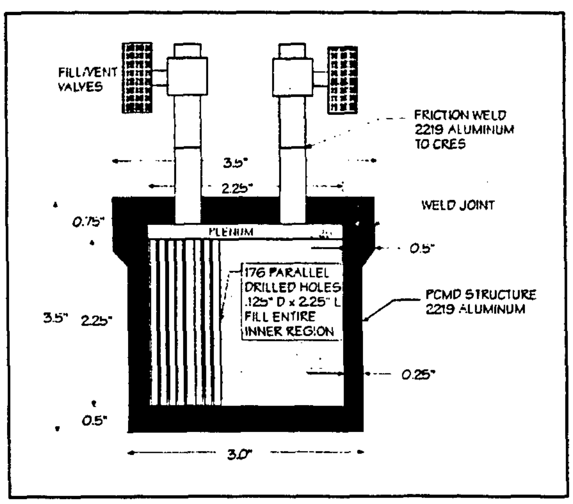

Figure 5. Prototype PCMD

The PCMD and cold head are connected via a 6061-T6 aluminum cold finger (Q-meter). Figure 6 illustrates the Q-meter design. In this proposal, Q-meter and cold finger are used interchangeably. The Q-meter shaft is 0.4" diameter by 3" long with circular 3" x .25" flanges on each end. Silicon diode temperature sensors are used to measure key PCMD and cold finger temperatures. Thermocouples are used to measure the $L\text{-}N_2$ shroud temperatures. Silicon diodes are

positioned on the cold finger top and bottom flanges and are used to measure the heat flow from the PCMD to the cold head. Silicon diodes are also positioned on the PCMD top and on the side of the PCMD very close to its bottom (near the cold finger top flange). A Kapton strip heater mounted to the top of the PCMD was used to simulate the sensor heat load. During Q-meter calibration, a different Kapton strip heater was mounted to the Q-meter top flange to simulate heat flow from the PCMD. Figure 7 illustrates the placement of the temperature sensors and heaters.

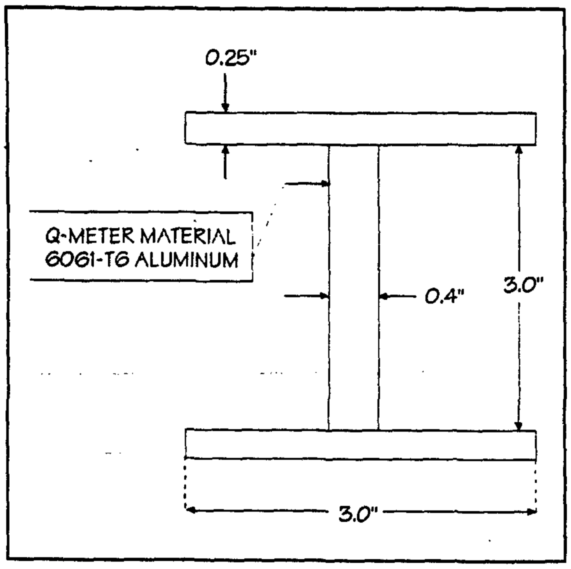

Figure 6. Q-Meter Design

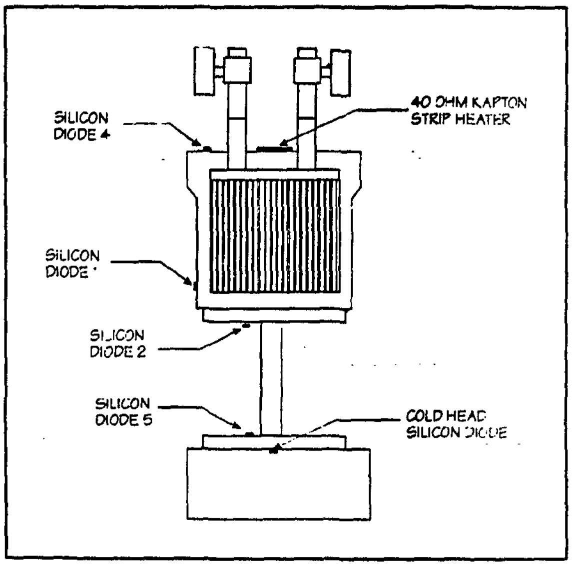

Figure 7. Temperature Sensor/Heater Placement

3.4 Simulation of Prototype PCMD and Test Apparatus

A 103-node SINDA'85 model of the PCMD and test set-up was developed. A melt/solidification model was developed and incorporated in the overall SINDA model. Calculations were carried out to assess prototype PCMD performance including structure temperature rise during phase change, temperature gradients within the aluminum structure, and temperature gradients within the fluid. Comparisons with an unfilled PCMD illustrate the impact of phase change. Additional calculations were performed for a PCMD placed on its side and a PCMD with 10 times the number of holes (at a constant total hole volume).

The results indicated that: (1) the 600 J PCMD prototype would release its phase change energy with a resulting structure temperature change of less than 1 K; (2) the maximum temperature gradient within the PCMD structure would be less than 0.5 K; (3) the maximum temperature gradient within the fluid would be approximately 0.75 K; (4) placing the device on its side rather than its nominal upright position will slightly enhance performance; and (5) increasing the number of holes by a factor of 10 (while keeping hole volume constant) will also enhance performance. Based on these preliminary results, the prototype PCMD and test set-up were expected to perform quite well. A more detailed description of the thermal model is provided in Appendix A. Additionally, listings of the SINDA'85 thermal model and the PCM melt model are provided in Appendices B and C, respectively.

4.0 Results

4.1 Q-Meter Calibration Test Results

A series of tests were conducted to calibrate the Q-meter for various cold head temperatures and heat flows. Cold head temperatures of 50 K and 75 K and heat flows of 1-4 W were utilized in the calibration tests. The liquid nitrogen shroud was not available during these calibration tests. The Q-meter was wrapped with 2 layers of two-sided aluminized Mylar insulation.

The tests were carried out by setting and maintaining the cold head at a constant temperature. With zero heater power the system was allowed to stabilize. Heater power was applied to the Q-meter top flange in 0.5 W increments. After each incremental increase in power, system temperatures were allowed to stabilize. Temperatures were recorded from the onset of the incremental power increase until temperature stability was achieved.

Figure 8 illustrates the Q-meter calibration results. In these curves the vertical axis is the difference between the cold finger top and bottom flange temperatures and the horizontal axis is the applied heater power. The slope of the curve is the cold finger resistance which turns out to be 8.33 K/W (about 0.12 W/K conductance). As seen, the Q-meter conductance is relatively insensitive to top and bottom flange temperature. With this conductance, a 1.0 W increase if heater power applied to the Q-meter top flange will increase the top flange temperature by about 8 K. In addition, extrapolating the calibration curves back to intersect with the horizontal axis gives the negative value of the parasitic heat gain (about 0.8 - 1.0 W).

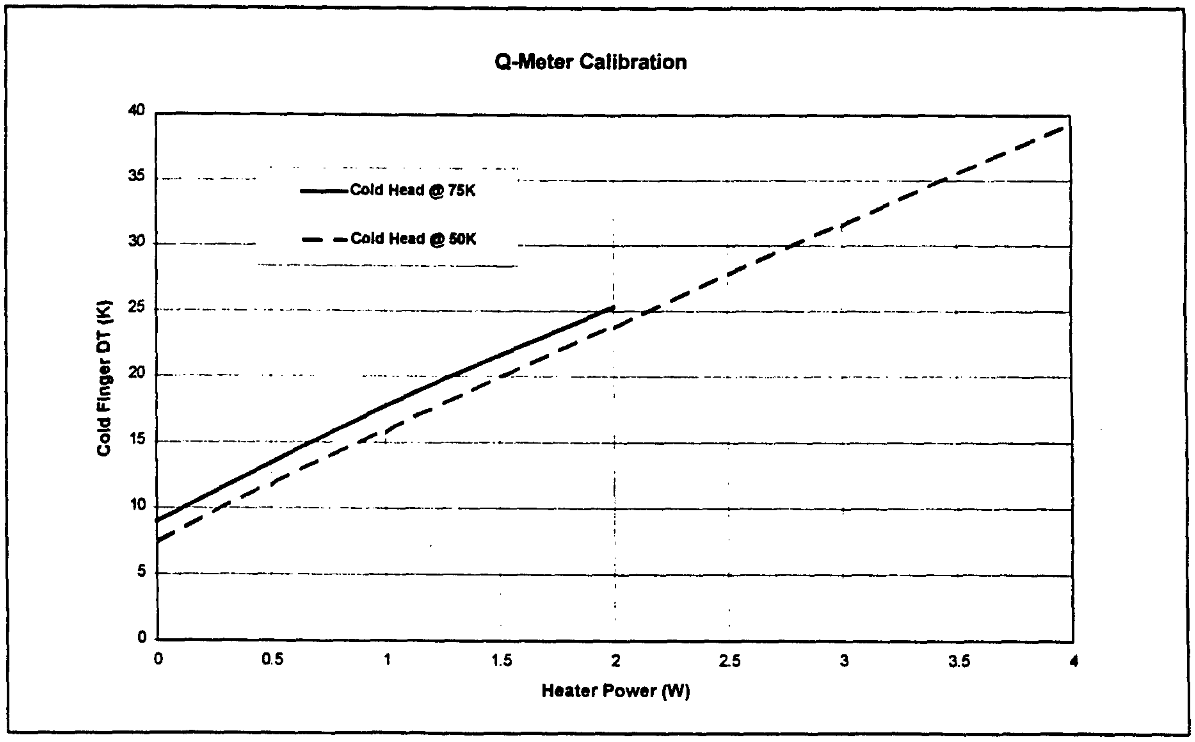

Figure 8. Q-Meter Calibration Results

4.2 PCM Characterization Test Results

A number of PCM characterization tests were conducted by Swales using the test apparatus described above. The tests summarized herein were conducted from 10/6/94 to 11/3/94. The PCMs that were tested include nitrogen, freon-22, air, and nitrogen trifluoride. PCMD heat-up and cooldown tests were conducted to ascertain transition temperature, supercooling behavior, and transition energy for each PCM as well as the isothermality of the PCMD. The characteristics of the tests conducted during the time period indicated above are summarized in Tables 2 and 3. During these tests, the liquid nitrogen shroud system was not fully operational, hence it was not used. However, the LN_2 shroud system will be used extensively during Phase II.

Table 2. Experimental Conditions for PCM Characterization Tests

PCM Tested	PCMD Fill Press. (psi)	MW (g/mol)	Fill Mass (g)	PC Energy (J/g)	Energy Storage (J)	Expected PC Temp (K) and Type
Nitrogen	3000	28	23.5	25.7	604	63.15, melt
Freon-22	Two-phase	86.5	75.8	?	?	59, s-s
Air	2000	29	16.2	23.1**	374	59, melt
NF_3	1100	71	21.8	21.3	464	56.7, s-s

* PCMD internal volume = 99.75 cc; ** Weighted average of N_2, O_2 values

Table 3. PCM Characterization and PCMD Performance Assessment Tests as of 11/3/94

Test #	Date	Test Type	Cold Head Temp (K)	Results Shown In	Comment
A	10/6/94	Q-Meter Calibration	75	Figure 8	
B	10/13/94	Q-Meter Calibration	50	Figure 8	
1	10/14/94	N_2 Heat Up	60	Figure 9	
2	10/14/94	N_2 Heat Up	60	Figure 9	
3	10/17/94	N_2 Heat Up	60	Figure 9	
4	10/17/94	N_2 Cool Down	35	Figure 10	
5	10/17/94	N_2 Heat Up	60	Figure 9	
6	10/17/94	N_2 Cool Down	35	Figure 10	
7	10/17/94	N_2 Heat Up	60	Figure 9	
8	10/17/94	N_2 Cool Down	40	Figure 10	
9	10/19/94	Freon-22 Heat Up	150	Figure 11	Freon 22 Melt Test
10	10/21/94	Freon-22 Cool Down	35	Figure 13	LN_2 Shroud Also Tested
11	10/22/94	Freon-22 Heat Up	38-50	Figure 12	
12	10/22/94	Freon-22 Cool Down	35	Figure 13	
13	10/23/94	Freon-22 Cool Down	30	Not Shown	Min. Steady-State Temp. Test
14	10/24/94	Freon-22 Cool Down	35	Figure 13	
15	11/1/94	Air Heat Up	55	Figure 14	
16	11/1/94	Air Cool Down	35	Figure 15	
17	11/1/94	Air Heat Up	55	Figure 14	
18	11/1/94	Air Cool Down	35	Figure 15	
19	11/3/94	NF_3 Heat Up	50	Figure 16	
20	11/3/94	NF_3 Cool Down	35	Figure 17	
21	11/3/94	NF_3 Heat Up	50	Figure 16	
22	11/3/94	NF_3 Cool Down	35	Figure 17	
23	11/3/94	NF_3 Heat Up	50	Figure 16	
24	11/3/94	NF_3 Cool Down	35	Figure 17	
25	11/3/94	NF_3 Heat Up	50	Figure 16	
26	11/3/94	NF_3 Cool Down	35	Figure 17	

Nitrogen Results

The N_2 phase transition was expected to occur at 63.15 K (via melting) with an energy of 25.7 J/gm. In these N_2 characterization tests, the PCMD was pressurized with to 3000 psi. The pressure was measured using the Linde gauge on our high pressure regulator. Using an internal PCMD volume of 99.75 cc, the ideal gas law (Equation (1)) indicates the N_2 mass within the PCMD to be 23.5 gms. To determine the energy storage capacity of this nitrogen-charged PCMD, the phase change energy is multiplied by the mass as indicated in Equation (2), yielding an energy storage capacity of 604 J.

$$m = PMV/RT = (3000/14.7)(1.01325E5)(28)(99.75E\text{-}6)/(8314)(295) = .0235 \text{ kg} \tag{1}$$

$$E_o = m \, \Delta H_m = (23.5)(25.7) = 603.95 \text{ J} \tag{2}$$

A total of eight tests were conducted to characterize N_2 as a PCM. These tests consisted of heating the system up through melt and cooling the system down through freezing. In the heat-up tests (Tests 1, 2, 3, 5, 7 as numbered in Table 2), net heating rates (heater + parasitics) of between 2-5 W were used to heat the PCMD through melt. In the cooldown tests (Tests 4, 6, 8), the cryocooler was set for maximum cooling yielding a net cooling rate of about 0.8 W. The results of Tests 2, 3, 4, 6, 7, and 8 are illustrated in Figures 9 and 10. In these figures, the temperature of silicon diode 1 (SD 1) is plotted for all tests and the temperature of silicon diode 4 (SD 4) is plotted for Tests 3 and 6. The difference between SD 4 and SD 1 represents the PCMD top-to-bottom temperature gradient (see Figure 7 for SD placement). As seen in the figures, silicon diode 4 runs roughly 0.3-0.5 K higher than silicon diode 1, a gradient that agrees with model predictions for comparable heat loads. Phase change is seen to begin at about 63.5 K on heating and 63.2 K on cooling. A more detailed assessment of the results is provided below.

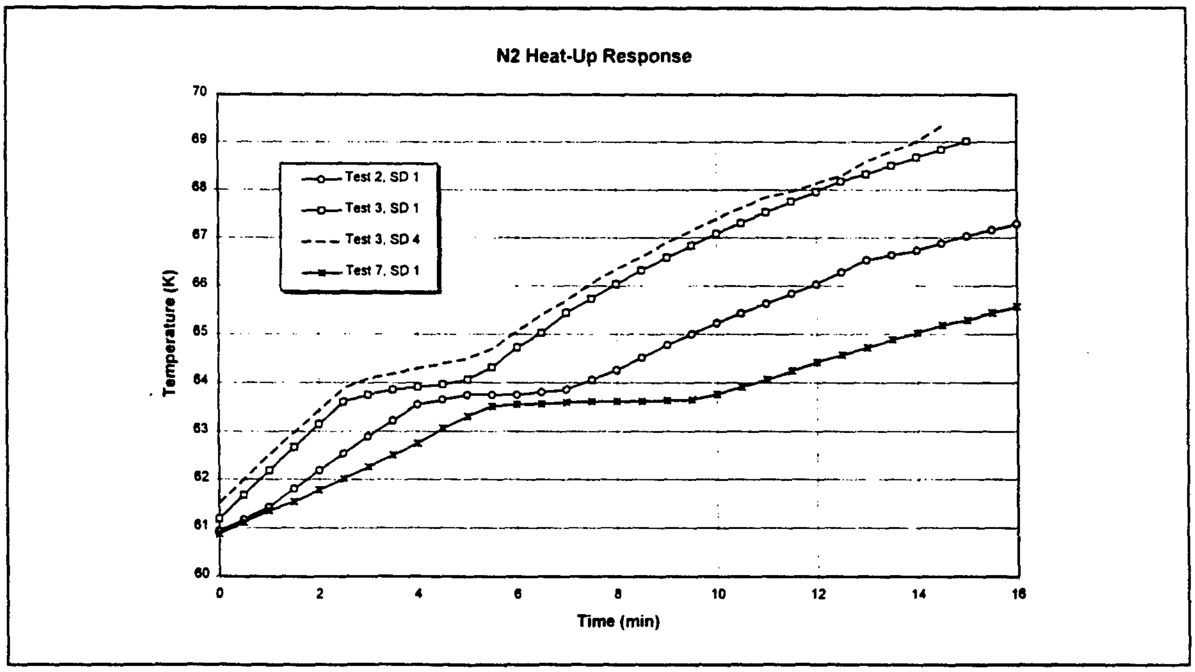

Figure 9. Nitrogen Heating Results

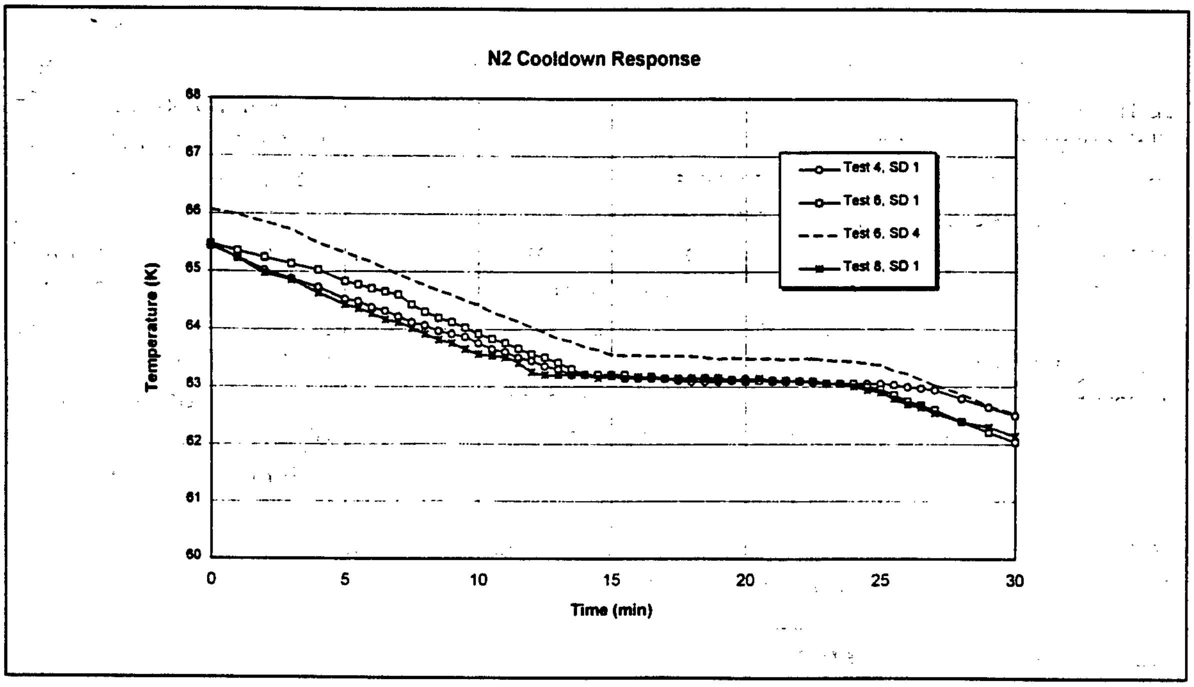

Figure 10. Nitrogen Cooling Results

The net heat flow into or out of the PCMD during phase change determines the phase change duration. The net heat flow (Q) can be approximated by multiplying the slope of the heating or cooling curves (DT/dt) just before phase change begins by mc_p, where m is the total mass and c_p is the average PCMD heat capacity (structure + fluid). The duration of phase change (Δt) is equal to the energy capacity of the PCMD divided by the net heat flow ($\Delta t = E_c/Q$). The heat capacity of aluminum at 63 K is 236 J/kg K. The heat capacity of solid N_2 at 63 K is roughly 1500 J/kg K. Since the PCMD weighs 1.0 kg, the value of mc_p for the PCMD at 63 K is mc_p = [(1)(236)+(.0235)(1500)] = 271.25 J/K. From Figure 9, DT/dt for Tests 3 and 7 just before phase change are 1.0 K/min and 0.5 K/min, respectively. Thus, Q is (271)(1)/60 = 4.52 W for Test 3 and (271)(.5)/60 = 2.26 W for Test 7. Using these net rates, the predicted phase change durations are 604/4.52/60 = 2.2 minutes for Test 3 and 604/2.26/60 = 4.4 minutes for Test 7. By looking at the length of the flattened slope regions in Figure 9, the measured phase change duration for Test 3 is about 2 minutes and that for Test 7 is about 4 minutes. So, the measured and predicted heat-up results are in good agreement.

The same procedure can be applied to the N_2 cooldown response curves in Figure 10. Here, DT/dt just preceding phase change is only about .175 K/min. Using the parameter values above, the resulting net cooling rate is (271)(.175)/60 = 0.79 W so that phase change should last for 604/0.79/60 = 12.7 minutes. Indeed, the phase change durations for Tests 4, 6, and 8 are between 11 and 13 minutes. Thus, the measured and predicted cool down results are also in good agreement.

In summary, N_2 and the prototype PCMD appear to function reasonably well as a thermal storage system. These characterization tests indicate that phase change begins at PCMD bottom temperatures of 63.2 K upon cooling and 63.5 K upon heating

with a maximum temperature change during transition of less than 0.5 K. Thus, supercooling does not appear to be a problem with N_2.

Freon-22 Results

The Freon-22 phase transition was expected to occur at 59 K (via solid-solid transition). The transition energy, however, was unknown. The PCMD was initially charged with 75.8 gms of Freon-22 and a total of six PCM characterization tests were conducted. To verify the charge mass, a Freon-22 melt test was conducted. Figure 11 shows the results of this melt test which indicates a strong phase transition at 116 K (literature value for T_{melt} is 113 K). The energy of this transition was backed out of the data yielding a value of 47 J/gm (literature value is 51 J/gm). The characterization tests consisted of heating the PCMD from well below to well above the transition temperature and cooling the PCMD in a similar manner. The results of these tests are shown in Figures 12 (heating) and 13 (cooling). Neither curve indicates the presence of an energetic phase transition phase transition at 59 K. Figure 12 may reveal the presence of a very weak transition that begins at about 52 K and ends at roughly 59 K as evidenced by a change in the slope of the heating curve. However, the results show that Freon-22 will not function acceptably as a 60 K PCM.

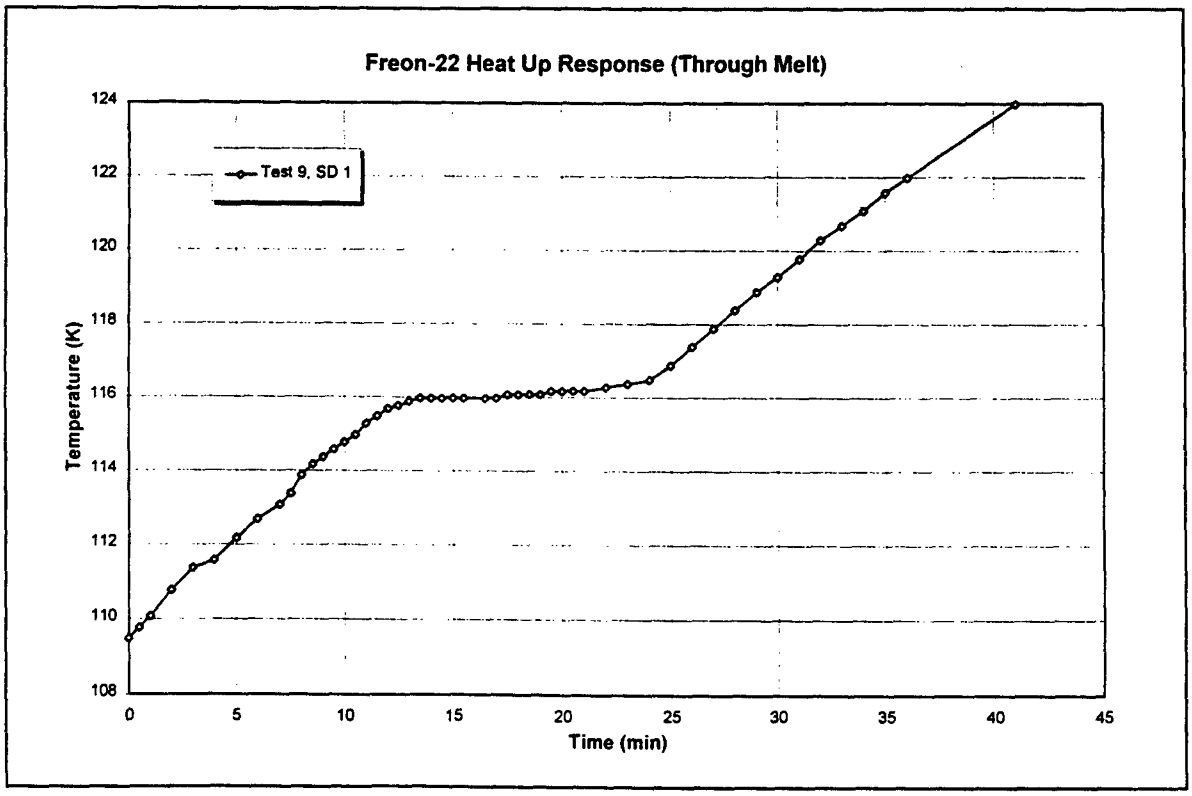

Figure 11. Freon-22 Melt Response

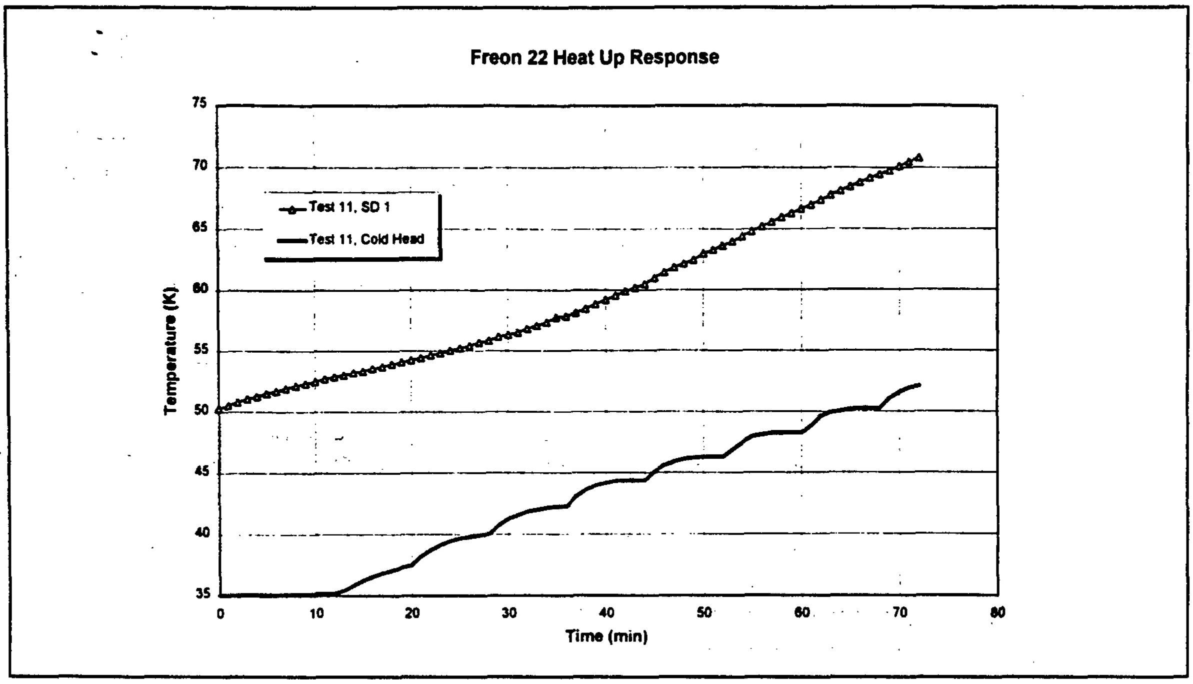

Figure 12. Freon-22 Heating Results

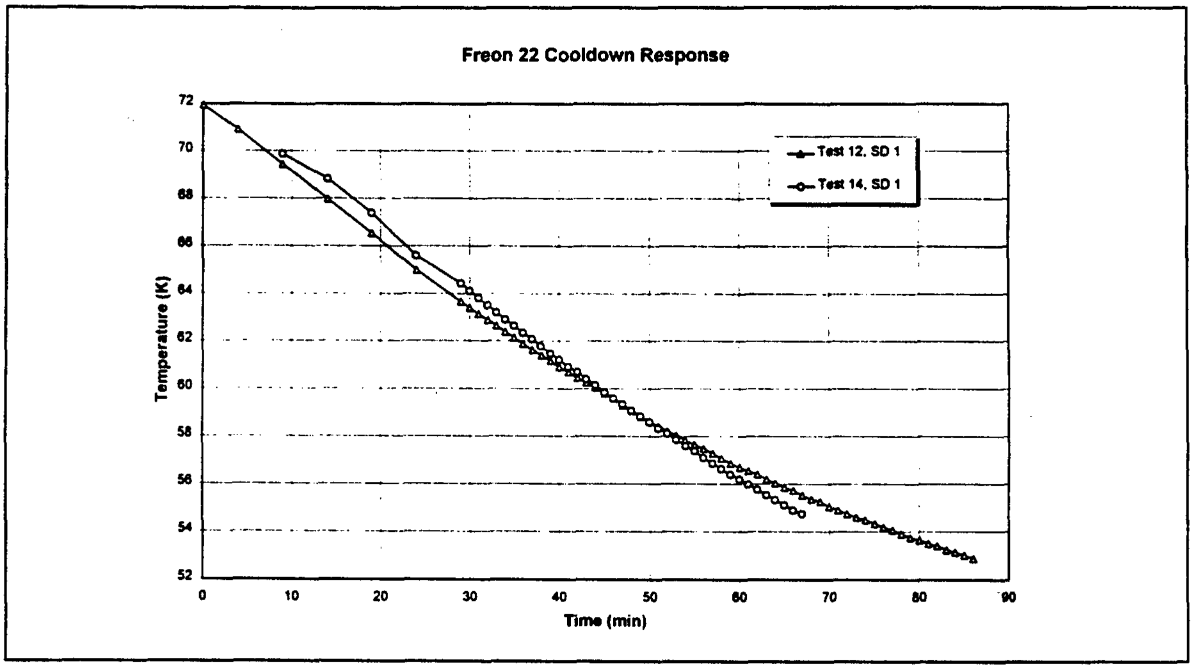

Figure 13. Freon-22 Cooling Results

Air Results

The phase transition for air was expected to occur at 59 K (via melting). Although the phase transition energy was not found in the literature, a 78% N_2 - 22% O_2 weighted average gives a probable transition energy of ΔH_{air} = (.78)(25.7)+(.22)(13.7) = 23.1 J/gm. In these tests, the PCMD was pressurized with air to 2000 psi. The resulting charge mass is calculated (by scaling the N_2 results) to be m = .0235(2000/3000)(29/28) = .0162 kg. So, the energy storage capacity of this air-filled PCMD is E_o = (23.1)(162) =

374.2 J. The heat capacity of aluminum at 59 K is 200 J/kg-K and it can be assumed that the heat capacity of solid air is roughly 1500 J/kg-K; that is, close to nitrogen value. Thus, the thermal capacitance of the air-filled PCMD is calculated to be $mc_p = (1)(200) + (.0162)(1500) = 224.3$ J/K. Applying the same procedure as indicated above for N_2, the phase change duration (Δt) can be computed by dividing the PCMD energy storage capacity (E_o) by the net heat flow (Q) into the PCMD during phase change ($\Delta t = E_o/Q$). The net heat flow is estimated by multiplying the PCMD thermal capacitance by the rate of change of PCMD temperature just before phase change ($Q = mc_p\ dT/dt$). The foregoing analytical relationships are applied below to analyze the air data.

A total of four tests (Tests 15-18) were conducted to characterize air as a 60 K PCM, and the results are illustrated in Figures 14 and 15. These figures indicate the presence of a phase transition for air which begins at about 58-59 K upon cooling and heating. From the cooling curves in Figure 15, the rate of change for Test 18 is roughly 0.25 K/min and that for Test 16 is about 0.067 K/min. These rates of change indicate phase change durations of 6.6 min for Test 18 and 24.8 min for Test 16. These predicted results agree roughly with the data, although compared to nitrogen, the duration of phase change for air is much more difficult to ascertain from the data. This difficulty is due partly to the fact the PCMD was charged with less air (thus the thermal capacitance of the PCMD masks the phase transition to a greater extent) and partly to the fact that air's phase transition temperature is probably is not as fixed as nitrogen's (thus, air probably melts and freezes over a temperature range rather than at a fixed temperature). Based on these results, one cannot rule out air as a 60 K PCM. More testing will be performed in Phase II.

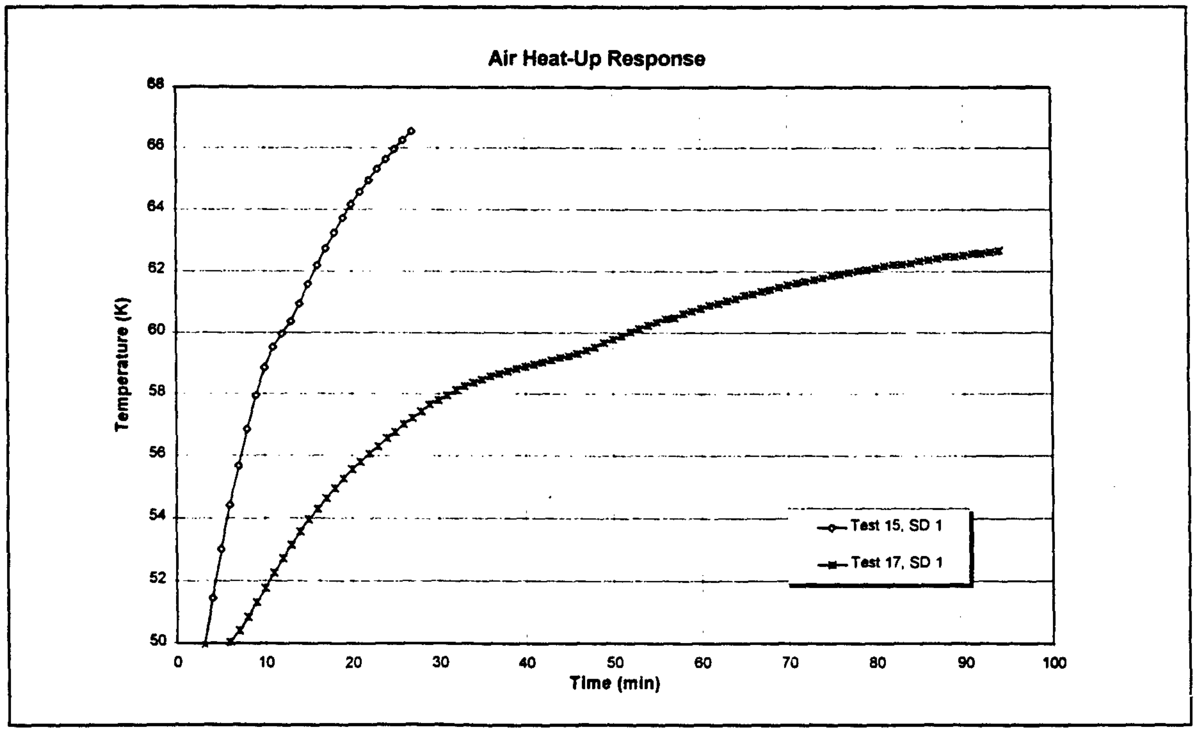

Figure 14. Air Heating Results

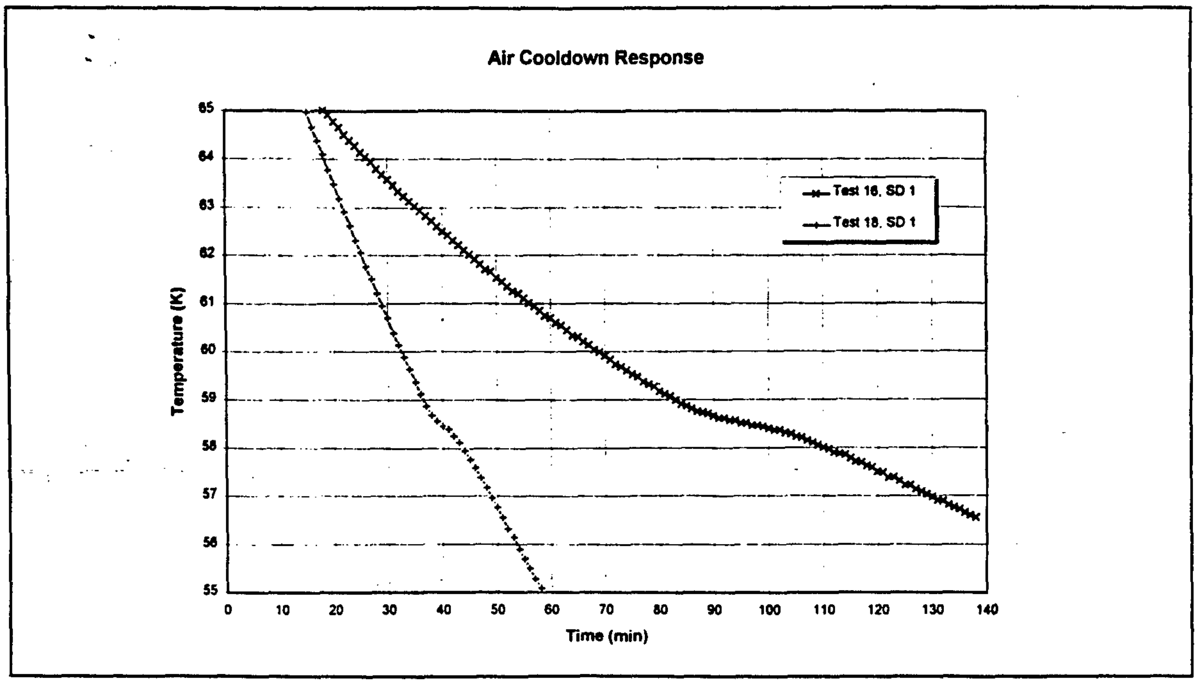

Figure 15. Air Cooling Results

Nitrogen Trifluoride Results

The phase transition for nitrogen trifluoride was expected to occur at 56.7 K (via solid-solid transition) with a transition energy of 21.3 J/gm. In these tests, the PCMD was pressurized with NF_3 to 1100 psi. The resulting charge mass is calculated (by scaling the N_2 results) to be m = .0235(1100/3000)(71/28) = .0218 kg. So, the energy storage capacity of this NF_3-filled PCMD is E_o = (21.3)(21.8) = 464.3 J. The heat capacity of aluminum at 57 K is 192 J/kg-K. Since data was not readily available, the heat capacity of solid NF_3 is assumed to be 750 J/kg-K; that is, about half the nitrogen value. Thus, the thermal capacitance of the NF_3-filled PCMD is calculated to be mc_p = (1)(192) + (.0218)(750) = 208.4 J/K. Applying the same procedure as indicated above for N_2 and air, the phase change duration (Δt) can be computed by dividing the PCMD energy storage capacity (E_o) by the net heat flow (Q) into the PCMD during phase change ($\Delta t = E_o/Q$). The net heat flow is estimated by multiplying the PCMD thermal capacitance by the rate of change of PCMD temperature just before phase change ($Q = mc_p\,dT/dt$). The foregoing analytical relationships are applied below to analyze the data.

A total of four tests (Tests 19-22) were conducted to characterize NF_3 as a 60 K PCM. The NF_3 results, which are illustrated in Figures 16 (heating) and 17 (cooling), turned out to be quite surprising. While Figure 16 shows typical PCM response -- that is, a flattened slope region during phase change -- Figure 17 indicates the presence of supercooling. In particular, whereas the solid-solid transition was expected to occur at 56.7 K, the cooldown curve shows that the transition does not occur until roughly 52-53 K, at which point an immediate rise in temperature of between 2.3 and 2.6 K takes place. Interestingly, the results show that the faster the cooldown rate the higher the transition temperature and the lower the amount of temperature rise, although these effects are not strong. This type of response is typical of supercooled materials, where

the material temperature falls below the transition temperature to the point where the supercooled condition can no longer be thermodynamically sustained, whereupon the material releases the excess energy (similar to an exothermic reaction) and the system rises in temperature in a very short period of time.

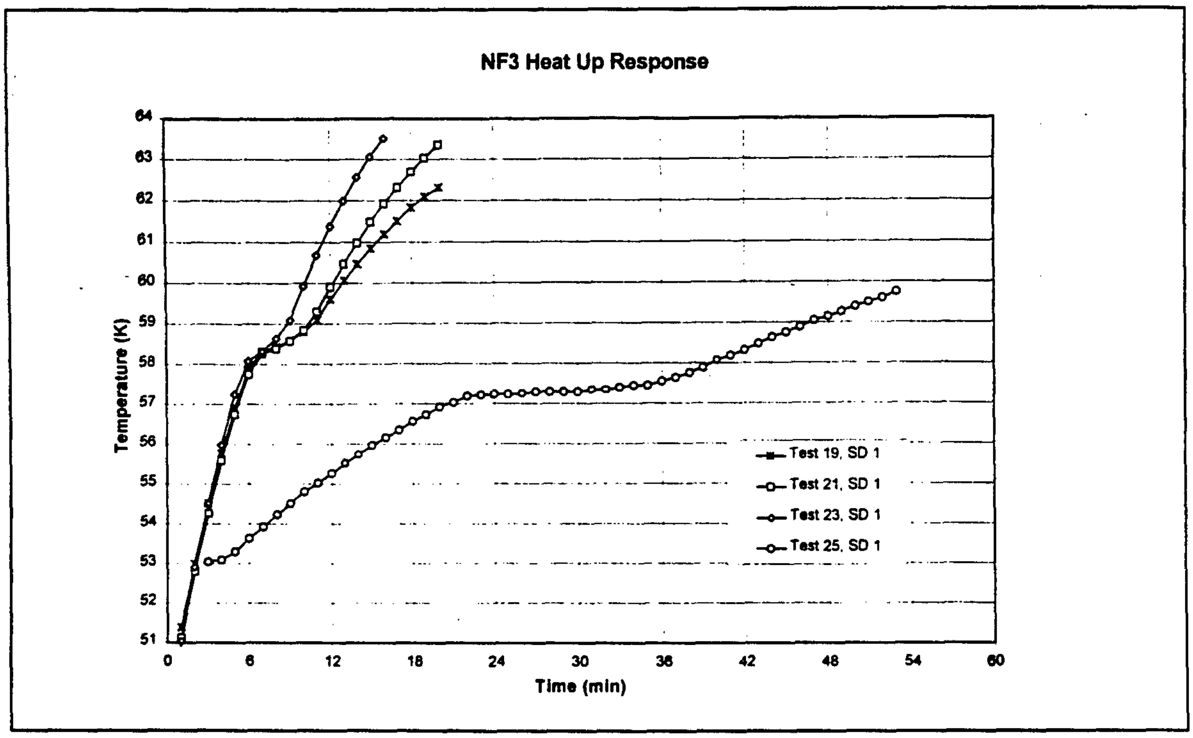

Figure 16. NF_3 Heating Results

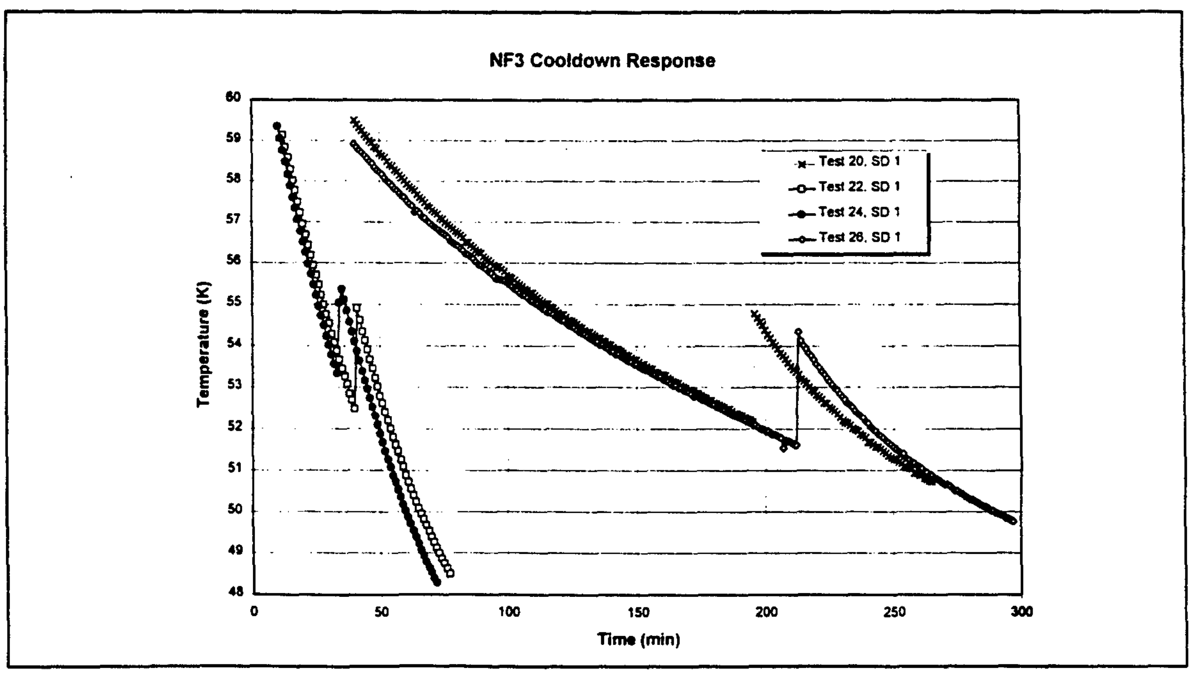

Figure 17. NF_3 Cooling Results

To determine whether the observed temperature rises are consistent with the NF_3-filled PCMD energy storage capacity of 464 J, a simple calculation can be performed for Test 20. The thermal capacitance (mc_p) of the NF_3-filled PCMD system at 57 K was calculated above to be 208.4 J/K. At 53 K, which is roughly the average temperature over which the 2.6 K temperature rise occurs (for Test 20), this value falls to 180 J/K. The energy released in this test is, therefore, E = (180)(2.6) = 468 J, which agrees very well with the calculated energy storage capacity value indicated above. To determine whether the duration of phase change seen in Figure 16 (for Test 19) is also consistent with this calculated energy storage capacity, the standard analysis procedure used to evaluate the other PCMs can be applied. In the Test 19 heating test, phase change begins at a temperature of about 58 K. The value of dT/dt just preceding phase change is roughly 1.0 K/min. This rate of change indicates the phase change duration should be 464/(1.0)/208 = 2.25 minutes, a result which is also in good agreement with the experimental data.

Based on the aforementioned results, NF_3 appears to be a very promising candidate for a 60 K PCM. In particular, if the observed supercooling behavior can be suppressed, and if a phase transition temperature of about 57 K is acceptable (the requirement is 60-65 K), then NF_3 offers some key advantages over nitrogen and air. The basic advantage of NF_3 over N_2 (and air) is that its high molecular weight increases the PCMD energy storage density (J/cc) by roughly (71/28)(21.3/25.7) = 2.10 times. Thus, for the same fill pressure and temperature, the NF_3-filled PCMD will have 2.10 times the energy storage capacity as one filled with nitrogen. As will be seen, these advantages will enable a scaled-up version of the prototype to meet flight requirements.

Summary of PCM Characterization Tests

To highlight the differences in heating and cooling response among the four PCMs tested, Figures 18 and 19 were prepared. Figure 18 illustrates the heating response and Figure 19 illustrates the cooling response of the four PCMs plotted next to one another.

4.3 Scaling-Up Prototype PCMD to Flight Unit

The prototype PCMD was designed to contain an internal pressure of 3000 psi with a safety factor of 2. To facilitate PCMD fabrication, no effort was made during Phase I, using structural optimization techniques, to minimize PCMD weight and/or maximize PCMD internal pressure capability. Additionally, no effort was made to optimize the void fraction in the interior core region while keeping PCMD thermal performance within requirements.

In Phase II, an NF_3-based flight PCMD will be designed based on the Phase I prototype design. The 6000 J flight PCMD (with NF_3 as the working fluid) would weigh about 3.0 kg, have an internal pressure at room temperature of 3000 psi, have an external volume of 1500 cc, and have an internal volume of 916 cc. The internal void fraction, as in the PCMD prototype, would be 50 percent. This device would be made out of 2219 aluminum (as the prototype was) and would have an outer diameter of 5.0", a height of 4.6", and a wall thickness of 0.4". In our engineering judgment, a 25 percent reduction in PCMD mass, and a 40 percent increase in PCMD internal pressure

capability, can be obtained by optimizing the structure while maintaining the current margin of safety. In addition, the internal working volume fraction can be increased by 50 percent and still perform effectively from a thermal standpoint. However, should these estimates prove to be unachievable, this scaled-up design meets all requirements. This optimized PCMD (consisting of 85% structure weight and 15% PCM weight) would have about four times the energy storage capacity of a 3 kg solid metal sensible heat device made out of Mg-Li alloy for a 1 K temperature rise. Figure 20 illustrates the weight savings of NF_3-based PCM storage vs. sensible heat storage with the Mg-Li high heat capacity alloy.

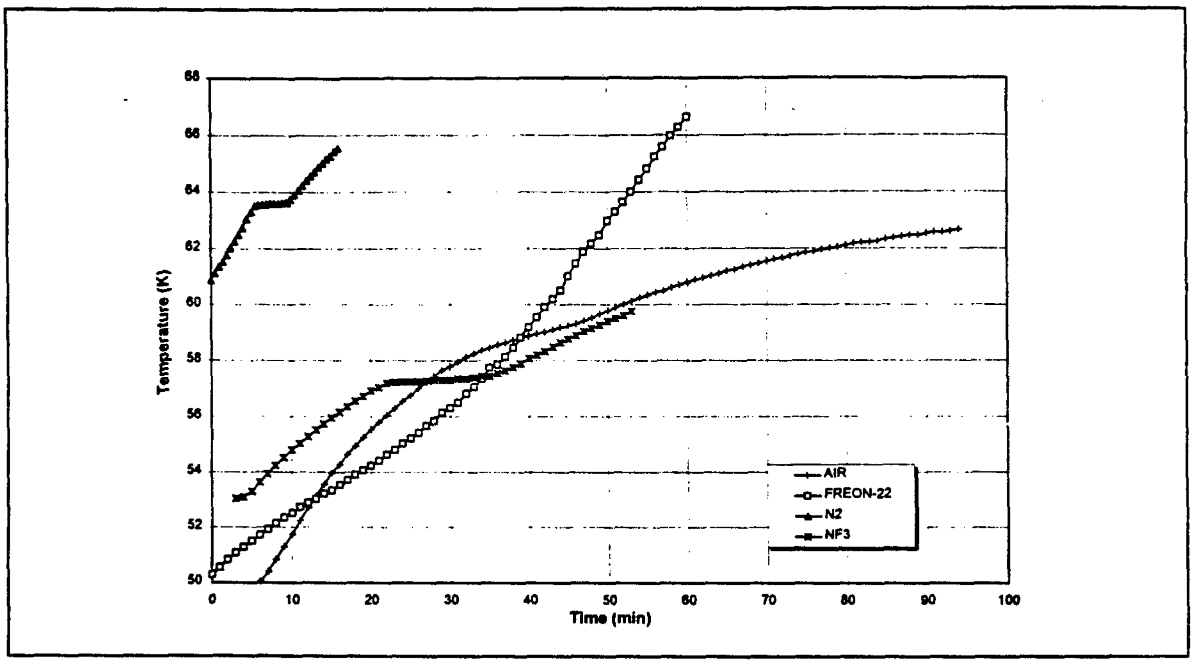

Figure 18. Comparison of Heating Results for N_2, Freon-22, Air, and NF_3

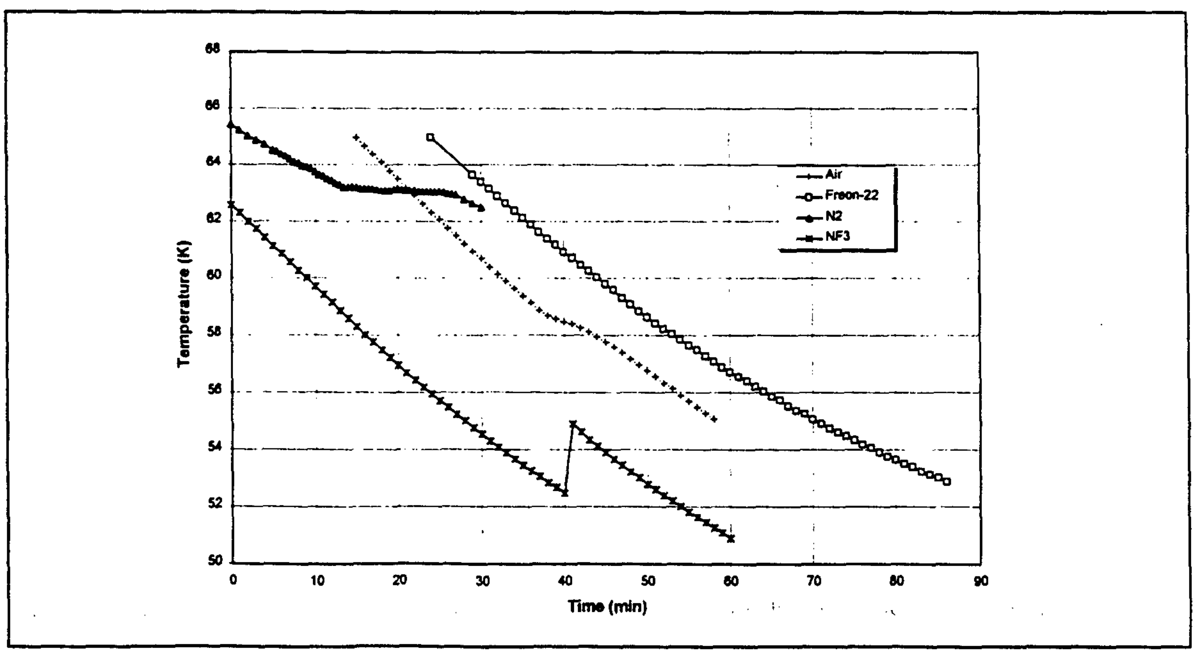

Figure 19. Comparison of Cooling Results for N_2, Freon-22, Air, and NF_3

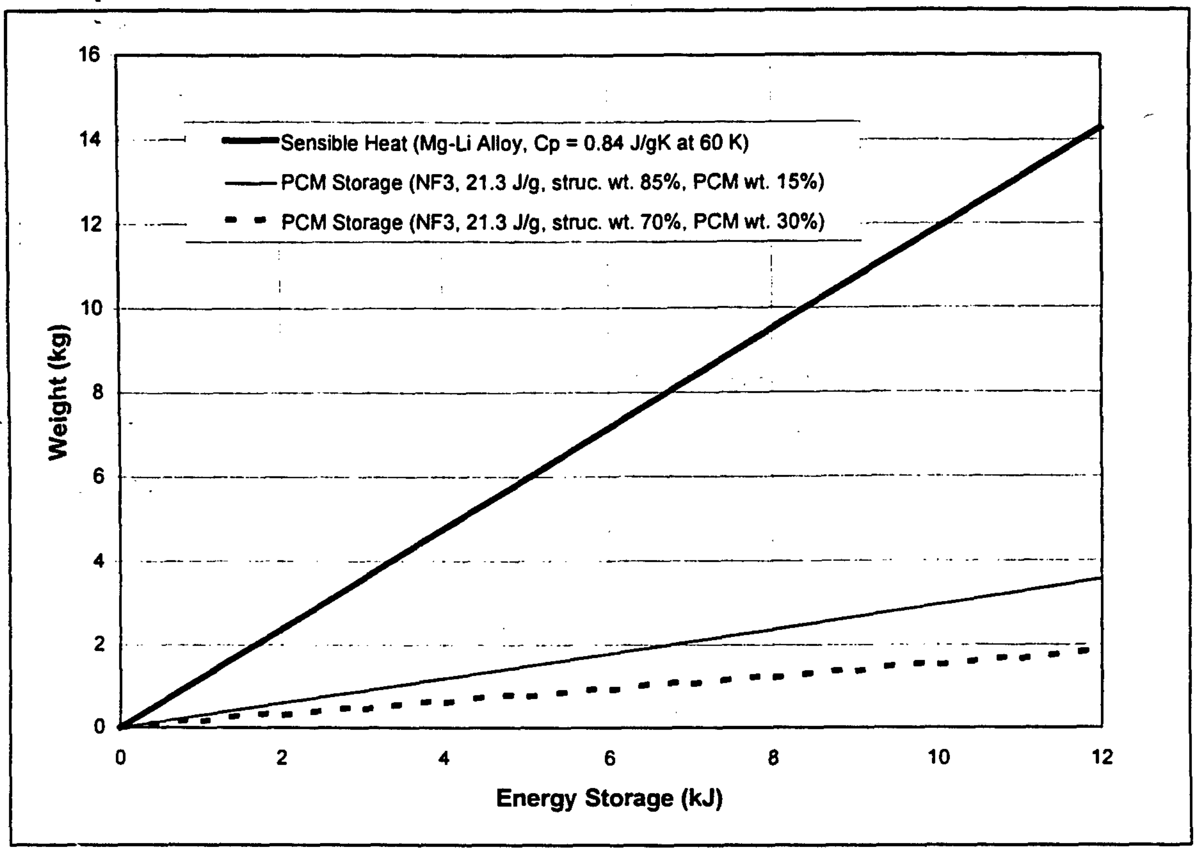

Figure 20. Weight Savings from NF_3 PCMD vs. High Heat Capacity Solid (Mg-Li Alloy)

5.0 Phase II Program

Our Phase II SBIR program objective is to develop a lightweight NF_3 60K phase change device. This development will provide a means to address and solve the problems associated with all phase change devices. Additionally, with the completion of the Phase II program, Swales will have a product (i.e., a lightweight, space-qualified cryogenic PCMD) that will be commercially marketable.

5.1 Program Overview

Given the successful Phase I demonstration of 60 K phase change feasibility, the fabrication of a prototype PCMD, the gathering of 60 K PCM performance data, and the scaling-up of the prototype PCMD to meet flight requirements, the following items will be accomplished in Phase II: (1) update the requirements for the 60 K PCMD -- this task will ensure that the Phase II product meets all current customer needs; (2) conduct appropriate analyses to optimize the PCMD design considering the size, weight, manufacturability, performance, cost, and risks of proceeding with the scaled-up design from Phase I vs. available design alternatives including the container structure material (metal vs. composite), the internal core design (integrated vs. separate core, holes vs. fins vs. metal matrix, etc.), heat input/output method (intrinsic conduction vs. heat pipes vs. conduction straps) -- keeping in mind that any PCMD must significantly outperform a

simple sensible heat device; (3) conduct critical component tests as required (e.g., PCM characterization tests and/or containment structure tests); (4) design, analyze, fabricate, and test a 60 K thermal storage unit (TSU) flight article -- performing all necessary thermal, structural, and safety analyses and tests; (5) design CRYOTP3 to test the TSU flight article including designing the coolers, structure, and electronics necessary as well as performing the required system vibration and thermal vacuum tests, supporting HH integration of CRYOTP3 into the STS, providing pre-launch, flight, and post-flight support, and supporting post-flight analysis and deintegration.

Our overall Phase II plan involves the technology development and commercialization of phase change technology. During the technology development portion, we will design a 60 K PCMD that meets the stated requirements, integrate this device, or a scaled version, into the CRYOTP3 experiment, and support a flight mission. Our commercialization efforts in Phase II will be directed towards developing a detailed commercialization plan, along with gaining commitments from potential customers for the application of our technology.

The results from Phase I are an integral part of the proposed Phase II program. Obviously, the demonstration of 60 K phase change and the PCM characterization data from Phase I are prerequisites to continuing the overall 60 K phase change SBIR program to Phase II and beyond. In addition, the test set-up constructed during Phase I, including the prototype PCMD, will be available to characterize additional fluids if such testing is required. This test set-up will also enable flight PCMD and flight Q-meter performance to be tested and verified. Additionally, the test set-up will enable quantitative trade tests to be performed quite easily if they are required. That is, if analysis results do not provide the needed confidence in a design modification or alternative, the test set-up offers the capability for conducting tests and gathering data to properly and fully answer any such performance trade-off questions. This capability may be quite useful if low temperature data for a promising composite container material or a promising core material is unavailable or highly uncertain. It would be very difficult to proceed with Phase II of this program without the information gained and the test equipment assembled during Phase I of the this SBIR program.

5.2 Flight Demonstration Opportunity

The flight PCMD and support hardware will be integrated into the CRYOTP experiment which will be installed within a HH-G canister on the STS. During Phase II we will design, analyze, fabricate, and test a 60 K thermal storage unit (TSU) flight article and perform all necessary thermal, structural, and safety analyses and tests needed to flight qualify the unit. In addition, the design of CRYOTP will be modified as required to accept this TSU flight article. The modifications to CRYOTP shall include designing/defining the coolers, structure, and electronics necessary as well as performing the required system vibration and thermal vacuum tests. The modified CRYOTP will be referred to as CRYOTP3. Finally, the effort will include supporting the integration of CRYOTP3 into HH-G and the HH-G/CRYOTP3 package into the STS, providing pre-launch, flight, and post-flight support, and supporting post-flight analysis and deintegration.

5.3 Phase II Technical Objectives

The technical objectives for Phase II consist of the following:

(1) Design a flight 60 K PCMD that meets all requirements
(2) Fabricate a flight PCMD and its support hardware
(3) Verify the performance of the flight PCMD in ground tests
(4) Modify the CRYOTP design to accept the flight PCMD and support hardware
(5) Demonstrate the performance of the flight PCMD in zero-G as a HH-G payload

5.4 Technology Issues

The key technology questions to be solved in Phase II relate primarily to optimizing the flight PCMD design, and are as follows:

(1) Can the scaled-up PCMD prototype be optimized to meet all requirements
(2) Is there a superior PCMD container material to 2219 aluminum (e.g. a composite)
(3) Is there an advantage to using a separate rather than an integrated core
(4) What are the trade-offs in using different types of core designs (e.g. fins vs. holes)
(5) Is there an advantage to using a heat pipe to transport energy to/from the PCM vs. relying on the intrinsic thermal conductivity of the container
(6) How can acceptable PCMD performance be assured in zero-G
(7) To what extent does PCMD shape, container material, core, and heat transport method impact the interfaces with the focal plane and the cryocooler in an actual IR sensor system

Clearly, not all of the above technology issues can be answered separately. Several of them must, in fact, be addressed from an overall system performance standpoint and this is what will be done during Phase II in arriving at an optimized flight PCMD design. In fact, one combination of alternative PCMD features may be competitive with the prototype design concept demonstrated in Phase I, and this alternative concept is illustrated in Figure 21 below. Some preliminary analysis work on the alternative concept indicated below has been performed to predict the performance of this concept. During Phase II, this design concept will be fully evaluated and quantitatively compared to the design approach already successfully demonstrated in Phase I.

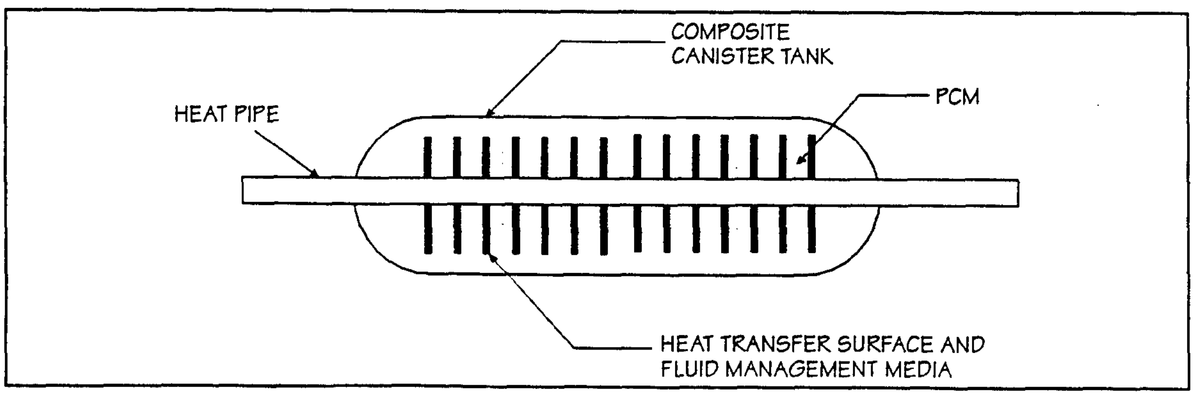

Figure 21. Alternative 60 K PCM Canister

5.5 Commercialization of PCM Technology

Cryogenic and high temperature phase change device technology can be applied over a wide range of very important commercial uses. As listed in Table 4, we have identified many potential commercial applications for PCMDs which range from high technology areas including microelectronics, supercomputers, microcomputers, earth resource satellites, communication satellites, medical devices, night vision sensors, and satellite thermal control, to lower technology applications including auto pollution control, enhanced coolant heat capacity, and personnel protection devices. This section briefly expands upon the aforementioned areas of commercial application and lists some of the vendors that will be contacted to discuss the commercial viability of these and other potential applications. During the initial part of the Phase II SBIR Program, we will narrow this list down to 2 or 3 of the most promising applications.

Computers\Micro Electronics. The operation of many microelectronic devices at cryogenic temperatures improves device performance, reliability, and lifetime. Ensuring the isothermality of the environment is also an important concern. Thus, an appropriately designed cryogenic phase change energy storage device could be used to level thermal loads associated with either cryogenic supercomputers and/or cold high performance microcomputer chips. Thermal coolers could be designed for peak efficiency at a specific load, and the load variations could be effectively "smoothed out" with the internal phase change of the device. For microprocessor chips, a miniaturized, low temperature phase change device could be incorporated directly onto the chip itself. We plan to contact Cray Computers, IBM, Texas Instruments, Cyrix, Motorola, Digital, AMD, and Intel to discuss the potential viability of these and other applications.

Earth Resource\Communication Satellites. The demand for mechanical coolers (e.g., Stirling cryocoolers) to provide and maintain long-life cryogenic operating temperatures for in-space electronic systems and sensors is continuing to grow. Important concerns for these systems include on-orbit temperature variability, due to internal and external environmental factors, as well as vibration minimization. To alleviate these potential problems while still receiving the long-life benefit of the mechanical systems, phase change device technology developed under government sponsorship can be transferred to the commercial sector. When developed, the phase change energy storage device could be used to either provide cooling for sensors with "zero" vibration and/or provide load-leveling cooling. To enhance system integrity, the energy storage device could be integrated directly into the sensor, focal plane and/or cooling system itself. We plan to contact Texas Instruments, Motorola, Hughes, Martin Marietta, TRW, and Loral to discuss the viability of these and other potential applications.

Medical Devices. An increasing number of medical devices (e.g., those based on SQUIDS) operate at cryogenic temperatures. Possible concerns in the operation of these devices include device nonisothermality and mechanical vibration, two areas where cryogenic phase change technology can provide benefit. Similar to the above applications, a cryogenic phase change energy storage device could be used to provide vibrationless cooling with load-leveling. In particular, medical device coolers could be designed for peak efficiency at a specific load, and the load variations could be

"smoothed out" with the internal phase change of the working fluid. We plan to contact Texas Instruments, Motorola, GE, and Siemens to discuss potential opportunities.

Night Vision Sensors. Night vision sensors require cryogenic operating temperatures and operate optimally when device temperature is relatively constant and vibration is minimized. As with the various applications mentioned above, an appropriately designed phase change energy storage device could be used to level thermal loads and minimize vibration associated with low temperature sensors. For CCD arrays, a cryogenic phase change device could be incorporated onto the CCD itself. We plan to contact Texas Instruments, Motorola, and Barnes Engineering to discuss potential opportunities.

Satellite Thermal Control. High power direct broadcast satellites, such as Teledesic, have short duty cycle, high power requirements. If current design practice is followed for these types of satellites, then large radiators, sized for the peak loads, will be required to dissipate the high peak power. Additionally some type of thermal control system will be required to maintain satellite temperatures during low power periods. The use of phase change devices, integral with the thermal control radiators, can potentially reduce the weight and cost of satellites that have short duty cycle, high power requirements. We plan to contact commercial satellite companies such as Teledesic, Loral and Martin to discuss potential opportunities.

Low Technology Applications. Phase change devices could be incorporated in to batteries to minimize the cold starting problems that occur in cold climates. Additionally, encapsulated phase change devices could be incorporated into fluid coolant and/or heating systems to help minimize the effects of peak loads. Finally, phase change devices could be incorporated in to personal protection devices for handling hot or cold materials. During the Phase II effort, we will investigate the potential for these types of devices by contacting companies such as Rheem, Trane, Carrier, Sears, Wal-Mart, K Mart, General Motors, Ford, and Chrysler.

Table 4. Potential Commercial Applications of The Phase Change Device

Application	Temp. Range (K)	Potential Customers
Earth Resource and Communication Satellites	40 - 150	TRW, Hughes, LMSC, Martin, OSC
Computers and Microelectronics	0 - 270	Cray, IBM, Intel, AMD, TI, Zilog, Motorola, Digital, Cyrix
Medical Devices	40 - 150	Siemans, Motorola, GE, TI
Night Vision Sensors	200 - 270	Motorola, Barnes Engineering, TI
Satellite Thermal Control	150 - 290	Teledesic, TRW, Hughes, LMSC, Martin, OSC
Low Technology Commercial Applications	200 - 290	Rheem, Trane, Carrier, Sears, Wal-Mart, K-Mart, GM, Ford, Chrysler

6.0 Phase II Work Plan

The Phase II work plan covers two main areas: (1) technology development and (2) commercialization. During the technology development part of Phase II, we will design a 60 K phase change device that meets the stated requirements, integrate this device, or a scaled version, into the CRYOTP3 experiment, and support a flight mission. Our commercialization efforts in Phase II will be directed towards developing a detailed commercialization plan, along with gaining commitments from potential customers for the application of our technology. All of the work described below will be performed by the SBIR Phase II team (see Section 9.0) at the Beltsville, MD facilities of Swales & Associates, Inc.. The following tasks will be performed in support of this effort. A detailed milestone chart (Figure 5-1) is provided in Section 5.4. The tasks to be completed during Phase II are outlined below.

6.1 Component Development

The objective of this task is to utilize the data gathered in Phase I to develop a 6000 joule 60 K device and, if necessary, a scaled version for the flight test. This effort is broken into the following sub tasks. With the completion of this task we will have a fully qualified 60 K PCMD design.

6.1.1 Update Requirements

The objective of this subtask is to refine the PCMD requirements outlined in Phase I. Additionally, the existing CRYOTP hardware will be reviewed to determine the requirements for a flight demonstration. With the completion of this subtask we will have a refined set of detailed requirements for the 6000 J PCMD and the any unique requirements for integration the PCMD into the existing CRYOTP.

6.1.2 Optimize TSU Design

The objective of this subtask is to conduct the appropriate analyses necessary to optimize the PCMD design considering the size, weight, manufacturability, performance, cost, and risks of proceeding with the scaled-up design from Phase I vs. available design alternatives. These alternatives include, but are not limited to, the container structure material (metal vs. composite), the internal core design (integrated vs. separate core, holes vs. fins vs. metal matrix, etc.), heat input/output method (intrinsic conduction vs. heat pipes vs. conduction straps). Additionally, during this subtask we will identify any critical/risk components for which thermal testing will reduce the risk to the program. With the completion of this subtask, the design requirements for a 60 K PCMD device, capable of dissipating a minimum of 6000 J, will be determined

6.1.3 Critical Component Tests

The objective of this subtask is to perform thermal testing of any mission critical or high risk components as determined in subtask 5.1.2. The testing will be performed using the test hardware developed during Phase I of the SBIR program. With the completion of this subtask the component level testing required to minimize program risk will be completed.

6.1.4 Design, Analyze, Fabricate, Test 60 K TSU Flight Article

In this subtask, the 60 K PCMD flight article (designated as the TSU) will be designed, analyzed, fabricated and tested so that it can then be integrated into the modified CRYOTP flight experiment. Modifications needed to CRYOTP to accept the 60 K device are outlined in the next subsection of this proposal.

6.2 Flight Demonstration

The objective of this task is to design and fabricate any additional CRYOTP flight hardware and support a flight test. This effort is broken into the following subtasks. With the completion of this task we will have demonstrated the performance of the 60 K PCMD device in the zero-G.

6.2.1 Design CRYOTP3

The objective of this subtask is to define the modifications necessary to the existing CRYOTP flight hardware to test the PCMD flight article. This includes the integration of new coolers, thermal insulation, low conductance support structure and any necessary structural modifications. With the completion of this subtask the modifications required to integrate the PCMD into the CRYOTP (hereafter referred to CRYOTP3) will be completed.

6.2.2 Incorporate TSU into CRYOTP3

The objective of this subtask is to integrate the TSU (i.e., the flight PCMD and supporting hardware) into the CRYOTP3 experiment. This effort will include performing the required system vibration and thermal vacuum tests. With the completion of this task, the PCMD and supporting hardware will be integrated into CRYOTP3.

6.2.3 CRYOTP Integration into Hitchhiker-G and STS

The objective of this subtask is to support the integration of the CRYOTP into a Hitchhiker GAS (HH-G) canister and the HH-G into the STS. This effort includes providing pre-launch, flight, and post-flight support, and supporting post-flight analysis and deintegration. With the completion of this task, the zero gravity performance of the PCMD will have been demonstrated.

6.3 Commercialization Plan

The objective of this major task is to develop a commercialization plan for marketing phase change devices. During this effort we will develop a plan and further identify and contact potential customers. With the completion of this task we will have developed and implemented a marketing plan.

6.4 Documentation

The objective of this task to write a final report detailing the entire Phase II effort.

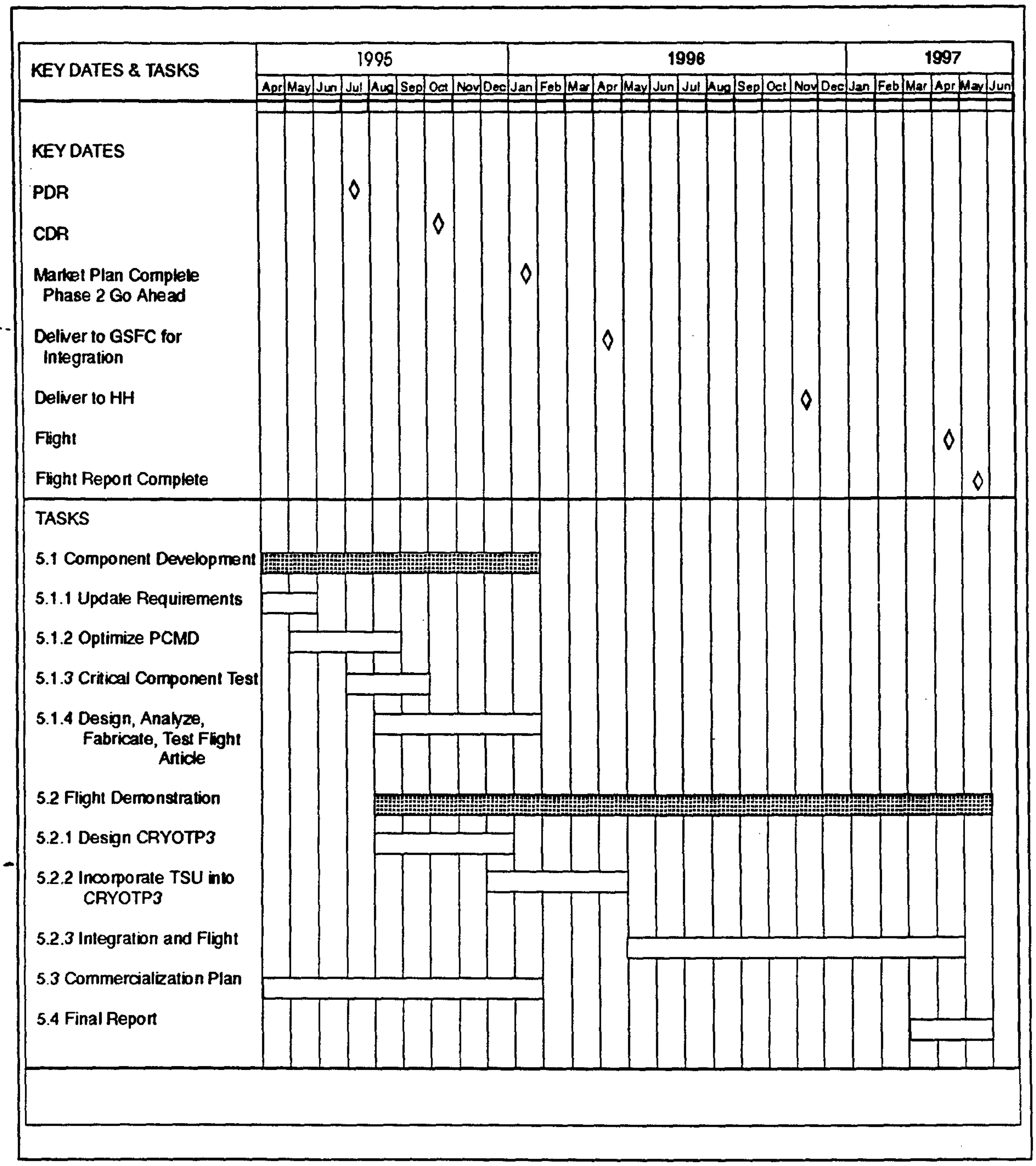

Figure 22. Schedule for the 60 K PCMD SBIR Phase II Program

7.0 References

[1] Knowles, T.R., "Cryogenic PCM Database", Preliminary draft report prepared by Energy Science Laboratories, Inc. for Grumman Space & Electronics Division, November 6, 1991.

[2] Grzyll, L.R., "Solid-Liquid Phase Change Materials Identification for Use Between 60 K and 65 K", Final report prepared for Swales & Associates, Inc. by Mainstream Engineering Corporation, August 2, 1994.

[3] Schultheiss, T., "Structural Analysis of the Brilliant Eyes Thermal Storage Unit (BETSU) for Hitchhiker", Report R-1-5257 prepared by Grumman Aerospace Corp., March 23, 1993.

[4] Brown, R., "Internal Thermal Model of the Brilliant Eyes Thermal Storage Unit (BETSU) PCM Canister", Grumman Aerospace & Electronics Memorandum ATSM-93-51, April 7, 1993.

[5] Brown, R., "External Thermal Model of the Brilliant Eyes Thermal Storage Unit (BETSU)", Grumman Aerospace & Electronics Memorandum ATSM-93-53, April 14, 1993.

[6] Bocchicchio, R.,"Brilliant Eyes Thermal Storage Unit (BETSU) Thermal Performance Test Plan for Flight Unit S/N 001", Report T-4-5257 prepared by Grumman Aerospace Corp., April 26, 1993.

[7] Alario, J., "Brilliant Eyes Thermal Storage Unit (BETSU) and Cryogenic Two Phase Flight Experiment (CRYOTP) Interface Control Document", Report ICD-5257 prepared by Grumman Aerospace Corp., April 26, 1993.

[8] Alario, J., "Brilliant Eyes Thermal Storage Unit (BETSU) Technical Requirements Document", Report TDR-5257 prepared by Grumman Aerospace Corp., May 28, 1993.

[9] Bugby, D.C., "Thermal Analysis of a Prototype 60-65 K PCMD and Test Set-Up", Preliminary analysis prepared by Swales & Associates, Inc., August 19, 1994.

Appendix A
Detailed Description of PCMD
Prototype Thermal Model

Introduction

This write-up describes the thermal modeling and analysis of the prototype phase change material device (PCMD) and test set-up. The calculations described in Appendix A were performed well before any test results were obtained and were performed using N_2 as the working fluid.

The PCMD was designed to provide approximately 600 J of fusion phase change energy using molecular nitrogen and other working fluids. The device is a cylindrical, 2219 aluminum pressure vessel with the following approximate dimensions: 3.0-3.5" outer diameter, 3.5" length, and 0.25-0.5" wall thickness. The device has a large internal surface area created by 176 internal 0.125" x 2.25" cylindrical holes which provide a high conductive coupling between the working fluid and the aluminum structure yielding nearly isothermal performance at or near 60 K. The aluminum structure weighs approximately 1 kg.

The PCMD test set-up utilizes an R.G. Hansen cryocooler to achieve the desired cryogenic operating temperature. The PCMD and cryocooler cold head are mounted within a liquid N_2-shrouded vacuum chamber to minimize radiation heat input. The PCMD and cold head and are connected via an aluminum cold finger/Q-meter. Temperature sensors on the cold finger and cryocooler cold head are utilized to control/measure the heat flow between the PCMD and cryocooler. A 1 W heater is used to simulate the sensor heat load.

A 103-node SINDA'85 model of the PCMD and test set-up was developed. A novel melt/solidification model was developed and incorporated in the overall SINDA model. Calculations were carried out to assess overall PCMD performance including structure temperature rise during phase change, temperature gradients within the aluminum structure, and temperature gradients within the fluid. Comparisons with an unfilled PCMD illustrate the impact of phase change. Additional calculations were performed for a PCMD placed on its side and a PCMD with 10 times the number of holes (at a constant total hole volume).

The results indicate that: (1) the 600 J PCMD prototype releases its phase change energy with a resulting structure temperature change of less than 1 K; (2) maximum temperature gradient within the PCMD structure is less than 0.5 K; (3) maximum temperature gradient within the fluid is approximately 0.75 K; (4) placing the device on its side rather than its nominal upright position will slightly enhance performance; and (5) increasing the number of holes by a factor of 10 (while keeping total hole volume constant) will also enhance performance. Based on these preliminary results, the prototype PCMD and test set-up are expected to perform quite well.

Model Description

A 103-node SINDA'85 model of the PCMD and test set-up was developed which includes 30 PCMD nodes, 7 cold finger nodes, 64 fluid nodes, a cryocooler cold head node, and a shroud wall node. A novel melt/resolidification model was developed and incorporated in the overall SINDA model. Provided below are detailed descriptions of the PCMD design, test set-up, and thermal modeling approach. The thermal modeling approach includes descriptions of the nodalization scheme, thermophysical properties, cryocooler performance, and the melt model.

PCMD Design

The design of the PCMD prototype is illustrated in Figure 5. The device is comprised of two 2219 aluminum sections which are welded together to form the pressure vessel. In the top section, two openings are provided for the fill/vent tubes. The fill/vent tubes are part aluminum and part CRES joined by friction welding. The aluminum ends of these tubes are welded to the PCMD top section. In the PCMD bottom section, 176 holes (.125" x 2.25") are drilled in a close packed pattern to provide a high surface area for heat transfer. A 0.25" gap between the top surface of the bottom section and the bottom surface of the top section creates a 20.1 cc plenum above the holes. The internal volume of the holes is 79.6 cc, thus the total working volume within the test PCMD is 99.7 cc. The overall device weighs about 1.0 kg not including valve weight.

To provide 600 J of phase change energy, the prototype PCMD must be filled at room temperature to a very high pressure. The device was designed for a burst pressure of 6000 psi so that it can be filled to 3000 psi with a safety factor of 2. To calculate the fill pressure, ideal gas behavior is assumed. The required nitrogen mass can be calculated by dividing the needed phase change energy (600 J) by the nitrogen heat of fusion (27,000 J/kg). Thus, a nitrogen mass of .0222 kg (22.2 gms) must be added to the device. The corresponding fill pressure is given by

$$P_{fill} = mRT/MV = (.0222)(8314)(295)/(28)(99.7E\text{-}6) = 1.95E7\ N/m^2 = 2830\ psi \qquad (1)$$

When the PCMD is cooled from this initial pressure down to 60 K, most of the nitrogen will solidify. The volume of solid will be about 22 cc since its density at that temperature is about 1 gm/cc. This result means that only the bottom portion of each hole will be occupied by solid nitrogen. Given a hole volume of 79.6 cc and hole length of 2.25", only the bottom 0.62" (2.25" x 22/79.6) of each hole will be occupied by solid nitrogen. Upon melting, the level will rise (about 20%) owing to the density change.

Test Set-Up

The overall layout of the test set-up is shown in Figure 3. As indicated in the figure, the test components consist of the cryocooler, vacuum chamber, pressure gauge, LN_2 tank and shroud, silicon diode reader, and computer control. The PCMD and cryocooler cold head are located within the vacuum chamber. In Figure 3, it is seen that the PCMD is attached to the cryocooler cold head via an aluminum cold finger. The

conductance of the cold finger at the operating temperature of the PCMD is about .12 W/K. Section 3.3 in the main body of the report describes the heater placement and instrumentation.

PCMD Nodal Diagram

The PCMD prototype is nodalized as shown in Figure A-1. A listing of the SINDA model is provided in Appendix B. The external PCMD structure is represented by nodes 201-206. The cold finger is represented by nodes 301-307. The internal PCMD structure is represented by nodes 1001-1008, 1011-1018, and 1021-1028. These 24 nodes divide the PCMD internal section into 3 axial sections, each with 8 equal thickness radial regions. For modeling purposes, the 176 holes are distributed within these radial sections based on cross sectional area. Thus, the number of holes within each radial section (from outer-to-inner section) are 41, 36, 30, 25, 19, 14, 8, and 3, respectively.

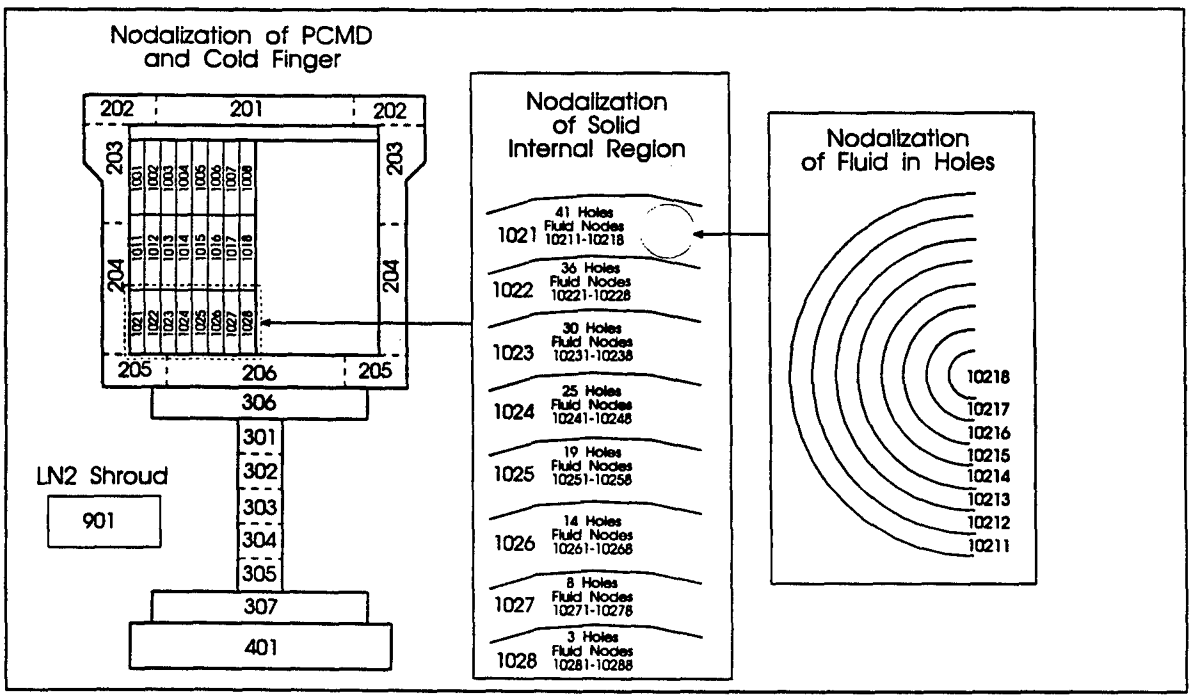

Figure A-1. PCMD Thermal Model Nodal Diagram

As indicated above, nitrogen is in contact with the bottom axial section, thus only nodes 1021-1028 are adjacent to fluid nodes. Within each of these radial regions, fluid temperatures within each hole are assumed identical and radially distributed across the hole. Thus, only one hole in each radial section needs to be modeled. Accordingly, nodes 10211-10218 represent the fluid within the holes in radial section 1021, nodes 10221-10228 represent the fluid in radial section 1022, etc. Only the outermost fluid nodes (10211, 10221, etc.) are in contact with the radial section node. By modeling heat transfer to/from one hole per radial section, the energy flow out of the radial section and into the fluid will be underpredicted. To account for this underprediction, the conductivity and heat capacity of fluid nodes must be multiplied by the number of holes.

This multiplication will not affect the internal temperature distribution within the fluid, but will increase the heat flow from/to the radial section.

Thermophysical Properties

The thermophysical properties used are contained within the HEADER ARRAY section of the SINDA input file listing at the conclusion of this Appendix. The heat capacity and thermal conductivity of aluminum are shown in Figures A-2 and A-3.

Cryocooler Performance

The cooling capability of the R.G. Hansen cryocooler is illustrated in Figure 4.

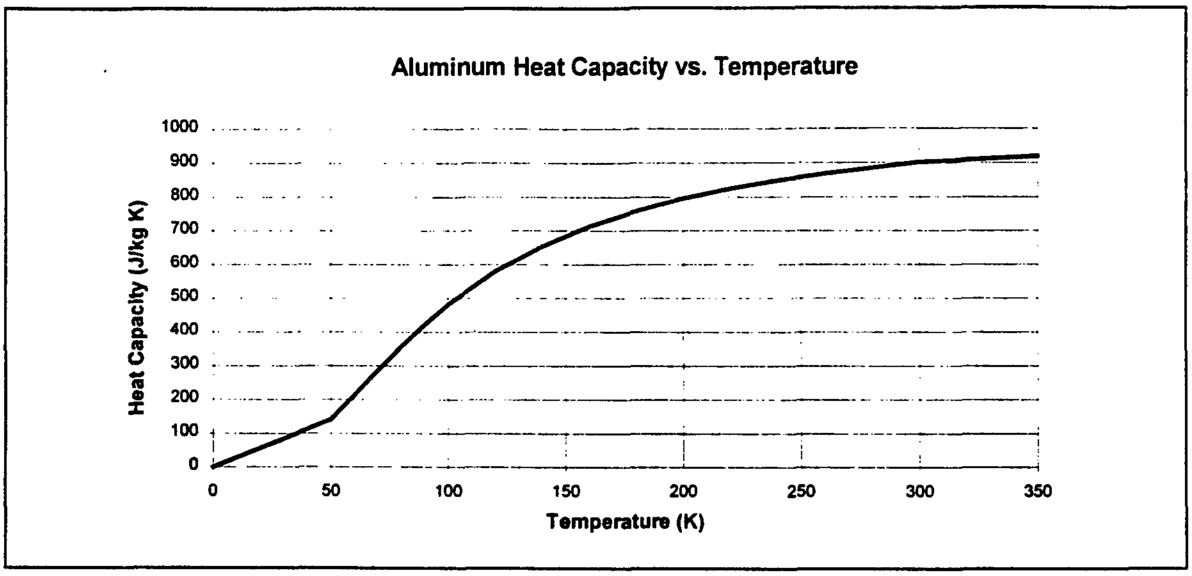

Figure A-2. Heat Capacity of Aluminum vs. Temperature

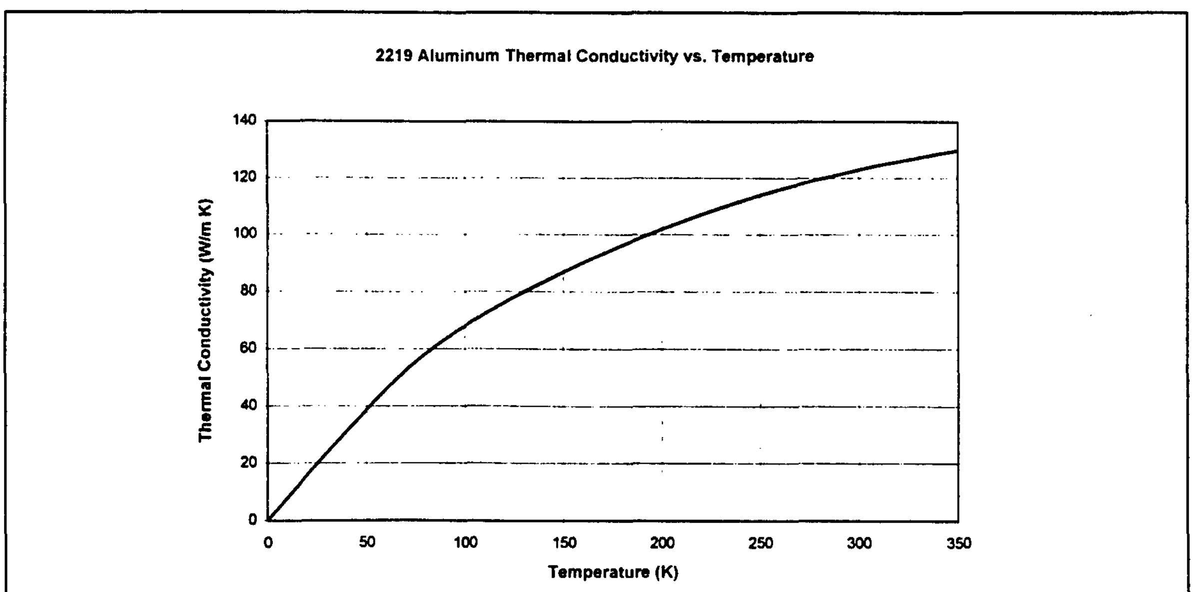

Figure A-3. Thermal Conductivity of 2219 Aluminum vs. Temperature

Melting/Solidification Model

The FORTRAN code used to simulate fluid melting within holes located in structure node 1021 is shown in Appendix C. This code, and similar code for radial sections 1022-1028, is incorporated into SINDA using INCLUDE statements. The basic model has the following features (T = fluid node temperature, c_p = fluid heat capacity, and T_{PC} = phase change temperature):

- There are 8 radial fluid nodes that can melt separately within each hole. The outermost fluid node is in contact with the aluminum in a given radial section.
- The fraction liquid ($F_L = 1 - E/E_o$) of each fluid node is computed to monitor the extent of melting/solidification process. E/E_o is the ratio of current/total phase change energy available (E_o is the phase change energy for holes in a given radial section and is based on the number of holes in that radial section).
- F_L is computed by performing a numerical integration: $F_L = F_L + \Delta F_L$. The change in liquid fraction ΔF_L is approximated at each time step by

$$\Delta F_L = -\Delta E/E_o = c_p\,(T_{PC} - T)/E_o$$

- To implement the above analysis, the following procedure is followed:

If $T < T_{PC}$ and $F_L > 0$ .... or .... $T > T_{PC}$ and $F_L < 1$

Then $T = T_{PC}$ and $F_L = \mathrm{Min}(1, \mathrm{Max}(0, F_L + \Delta F_L))$

Results

The results presented below include descriptions of the calculation sequence, the cases simulated, some anticipated results from hand calculations, and the temperature-time plots.

Calculation Sequence: The PCMD test simulations were carried out using the calculation sequence described below. Phase change occurred during cool-down and heat up as the fluid temperature passed through 63 K.

- Each calculation begins at an initial temperature of 70 K. About 2 hrs would normally be required to transition from room temperature to this temperature level.
- The cryocooler operating temperature is initially set to 35 K (maximum cooling).
- The system cools down until a calculation time of 0.5 hrs is reached. At that time, the cold head set point is increased to 58 K.
- Between 0.5 and 1.0 hrs, the cold head is maintained at 58 K.
- At a time of 1.0 hrs, the 1 W sensor simulator heater (on node 201) is enabled and the cold head set point tracks the cold finger top flange temperature (node 306).
- When a time of 2.5 hrs is reached, calculations cease.

Cases Simulated: The following four cases were simulated: (1) *Baseline* -- PCMD positioned as shown in Figure 4 (upright); (2) *No Fluid in PCMD* -- a case was run with the nitrogen removed from the device; (3) *On Side* -- PCMD positioned on side (to increase contact area, conduction in holes); (4) *Increased Hole Number* -- Number of holes increased by 10X at fixed hole volume.

Anticipated Model Results from Hand Calculations: The following calculations are applicable during the heat up portion of the simulation. With a total phase change energy of 600 J and an input power of 1 W, the duration of phase change during heat up should be about 600 seconds (.167 hrs). The structure temperature change during phase change (assuming the structure is isothermal) can be estimated by looking at heat transfer within a fluid hole during melting. The energy flow into a single hole is Q = 1/176 = .0057 W. Within each hole, 95% of the fluid mass is contained between the outer radius r_o and an internal radius of $.22r_o$. The conductance across an annulus of outer radius r_o and inner radius $.22r_o$, and which is .62" thick, is given by $G = 2\pi kL/\ln(r_{outer}/r_{inner}) = 2\pi\ (.13)(.62/39.37)/\ln(1/.22) = .00849$ W/K. Thus, the maximum temperature change which is anticipated to occur in this prototype PCMD during phase change is $\Delta T = Q/G = .0057/.00849 = 0.67$ K (note: the thermal conductivity used for solid/liquid N_2 was .13 W/mK).

Temperature-Time Plots: The following plots were generated to illustrate the predicted performance of the prototype PCMD. In Figure A-4, the temperature of node 201 is shown for the baseline and no fluid cases to illustrate the significant impact of phase change on PCMD thermal response. In Figure A-5, the temperatures of nodes 201, 206, 1001, 1008, and 1028 are shown to illustrate temperature gradients within the PCMD structure. In Figures A-6 and A-7, the temperatures of nodes 10211, 10218, 10281, and 10288 are shown to illustrate temperature gradients within the fluid. Lastly in Figure A-8, The temperature of node 201 is shown for the four simulated cases.

The aforementioned figures indicate the following:

- A distinct reduction in dT/dt for the PCMD structure is evident as the PCMD temperature passes through 63K on cooldown and heat up. This behavior indicates that phase change will be easily seen during the upcoming tests.
- The duration of this reduced slope region during heat up is roughly .16-.18 hours which is consistent with the hand calculations (see Figures A-4 to A-8).
- The maximum structure temperature change during phase change in about 0.75 K, which is consistent with the hand calculations (see Figure A-4).
- The entire PCMD structure is nearly isothermal (see Figure A-5).
- The maximum temperature gradients within the fluid are about 0.75 K which is to be expected since this gradient drives the change in structure temperature during phase change (see Figures A-6 and A-7). This result is also consistent with the hand calculations.

- Laying the PCMD on its side will enhance performance slightly by reducing the temperature gradients in the fluid which reduces the structure temperature change during phase change (see Figure A-8).

- Increasing the number of holes by a factor of 10 while keeping the working volume constant will also enhance performance for the same reason as indicated above (see Figure A-8).

<u>Conclusion</u>

The basic conclusion of this analysis is that the prototype PCMD as currently designed will perform quite well. In particular, the results show that the design will provide 600 J of nearly isothermal phase change energy at 63 K. The results also indicate that the test set-up as currently configured will provide an effective means to experimentally demonstrate PCMD performance. As a check on the SINDA model and results, a few key hand calculations were performed. The results of the hand calculations were consistent with the SINDA results. The next step, therefore, is to begin testing the prototype PCMD.

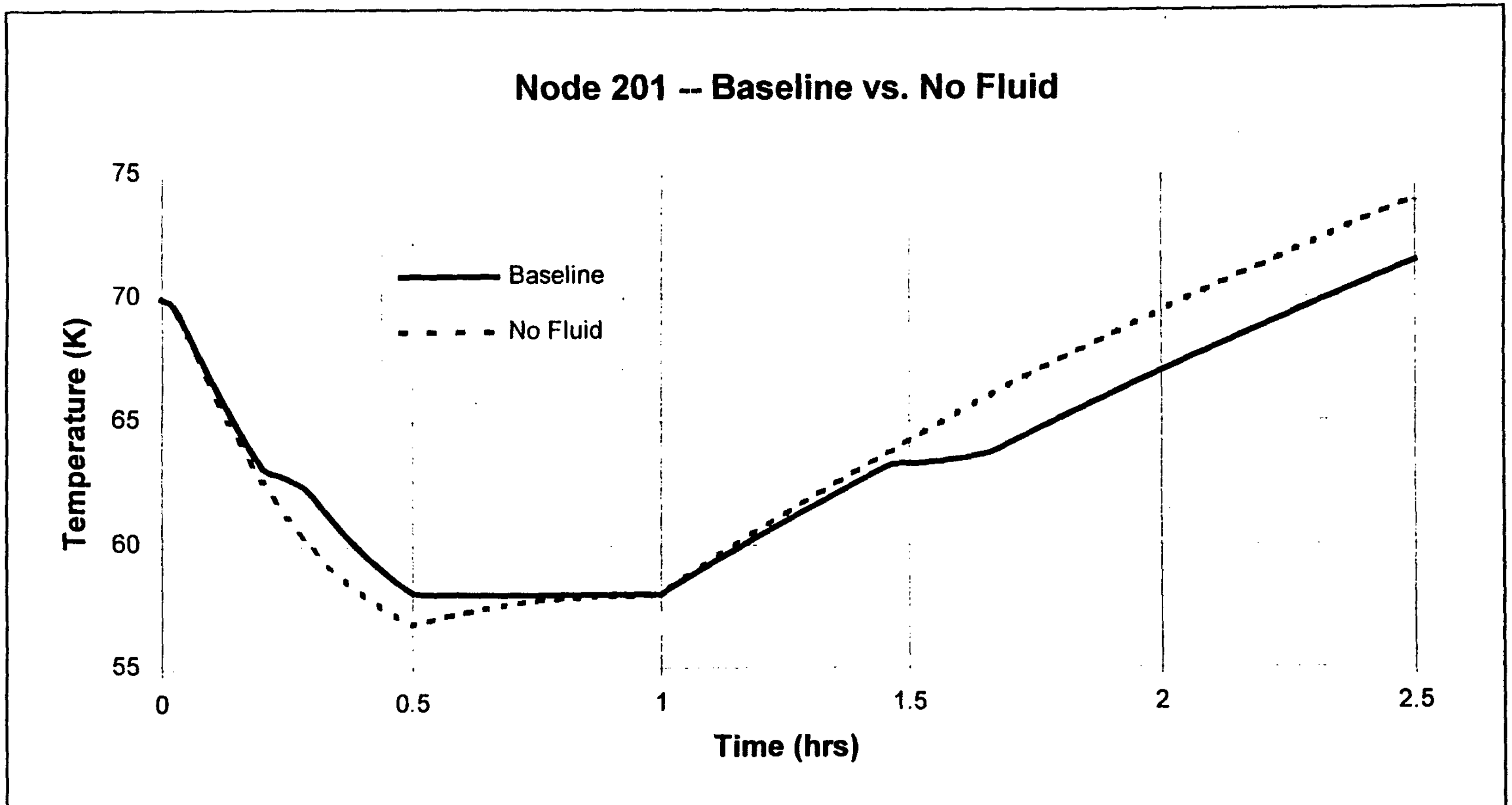

Figure A-4. Baseline Results for PCMD Node 201 vs. Case with No Fluid

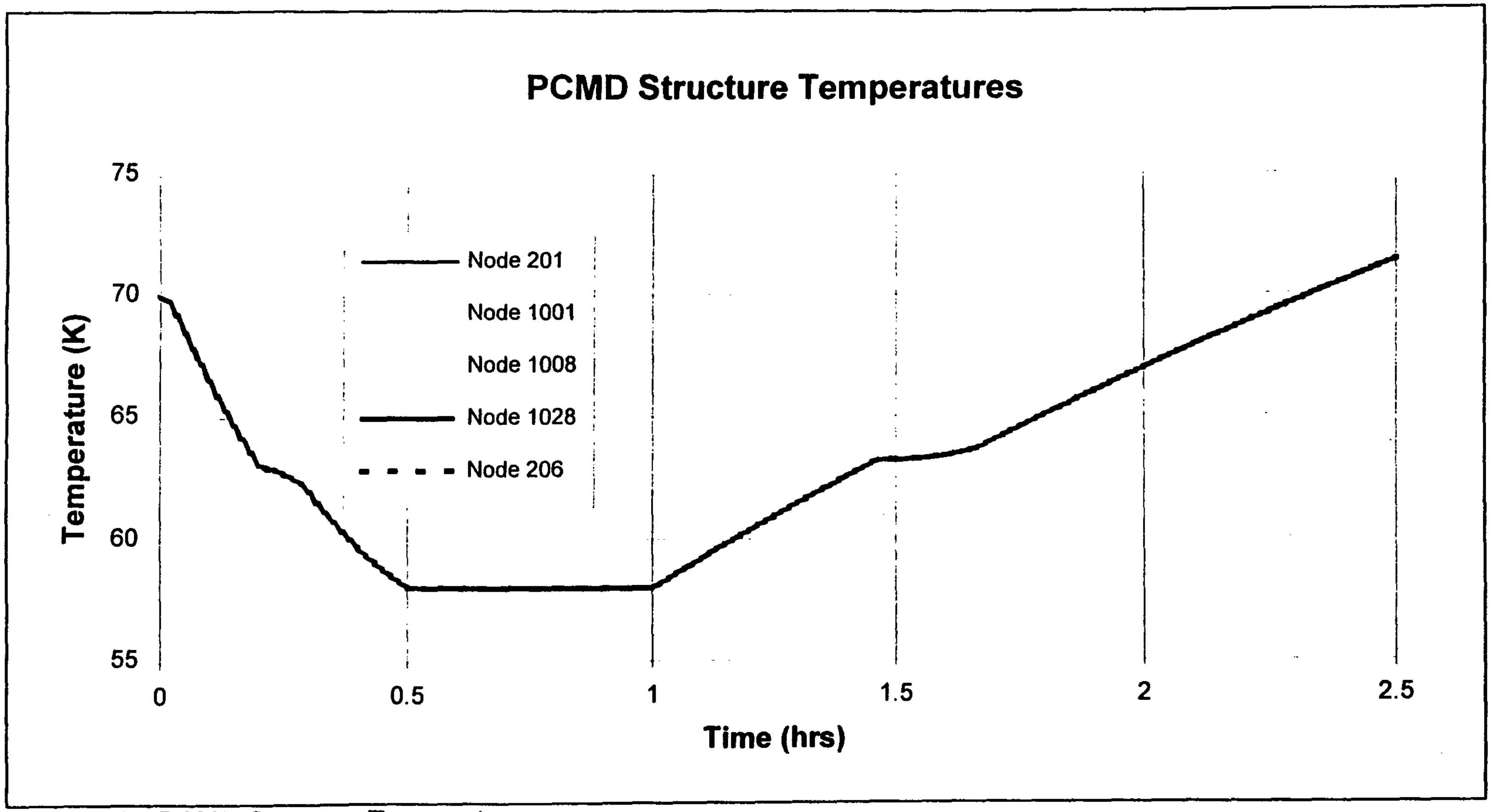

Figure A-5. PCMD Structure Temperatures

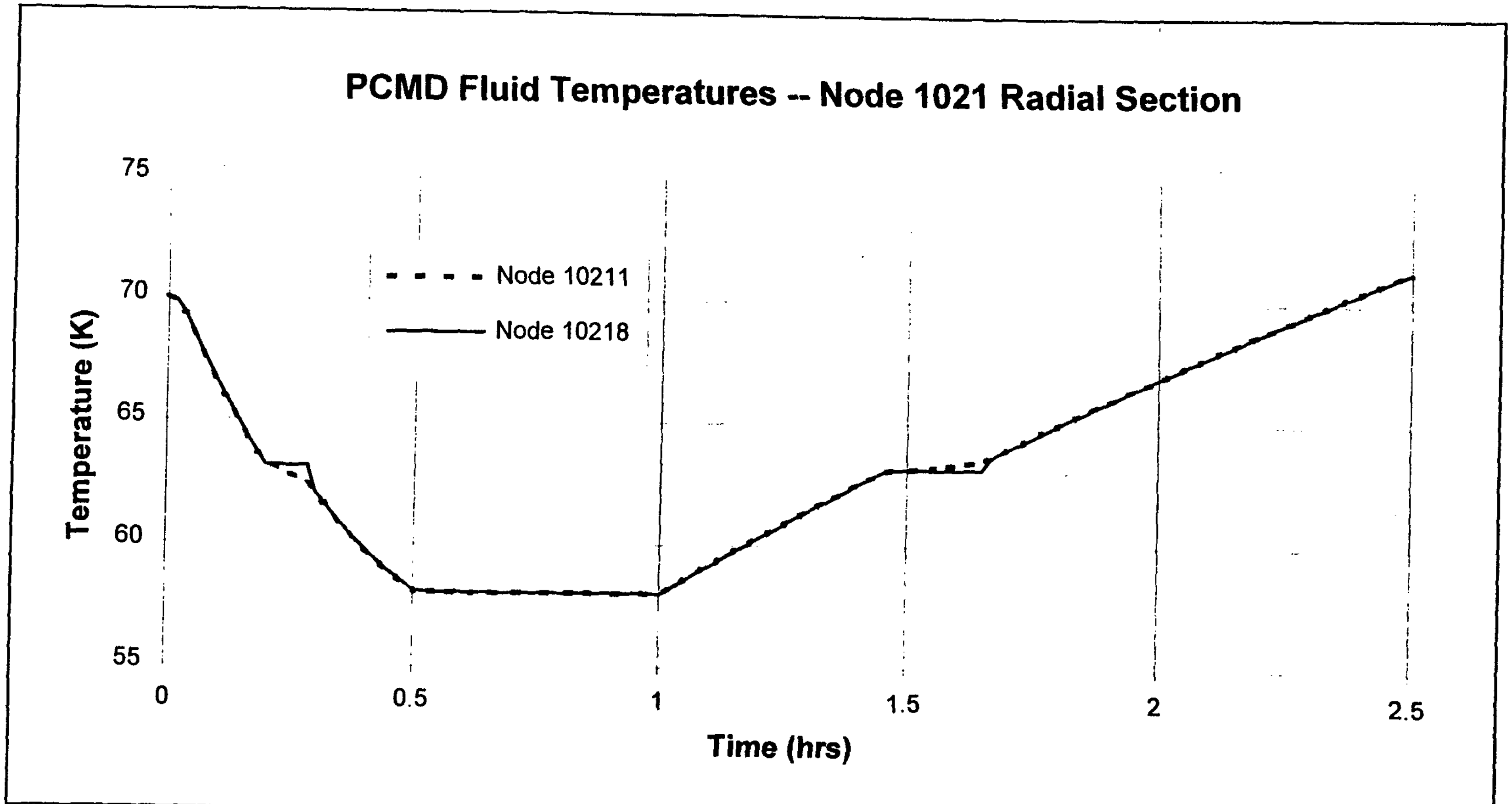

Figure A-6. PCMD Fluid Temperatures -- Node 1021 Radial Section

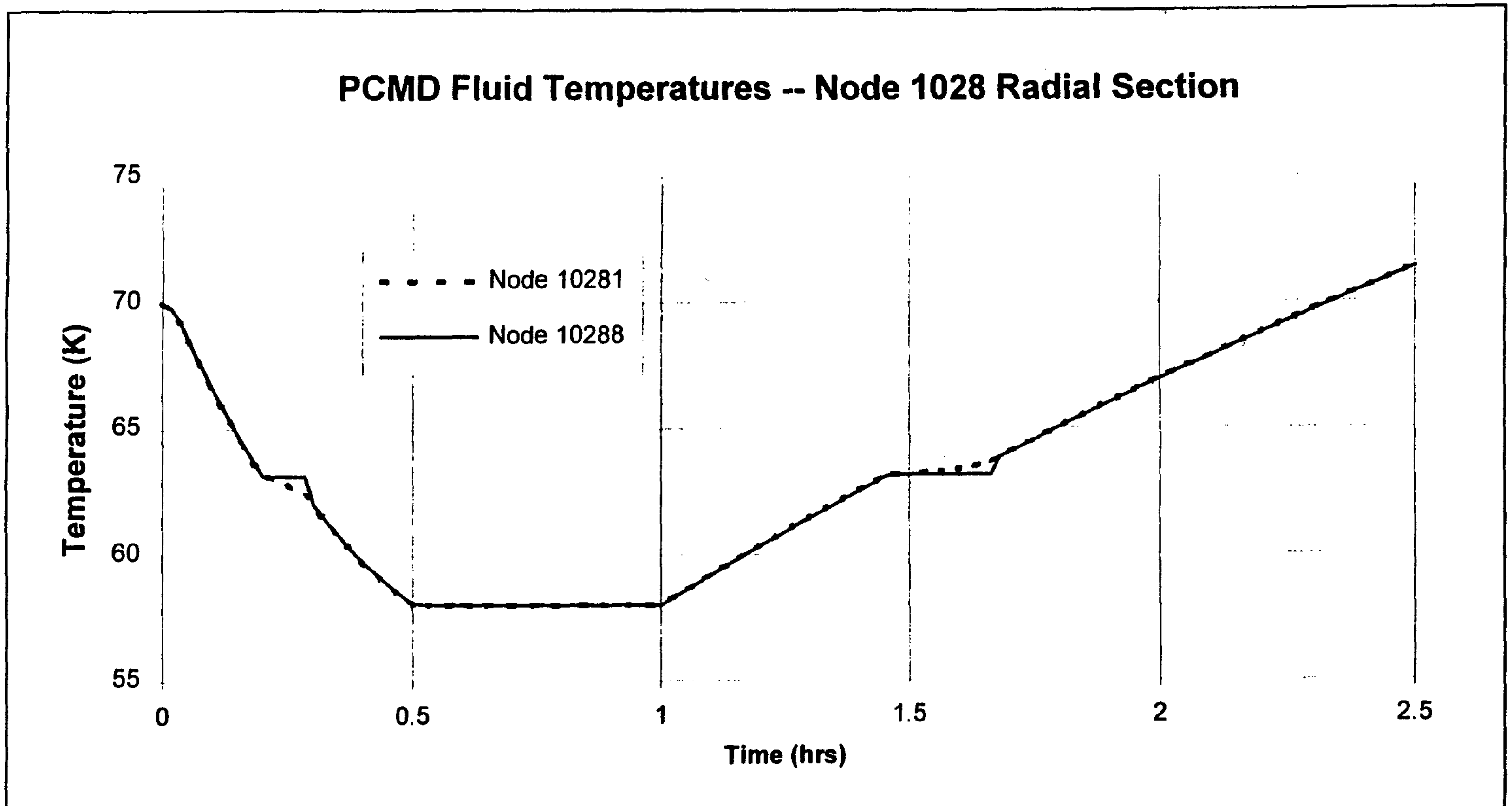

Figure A-7. PCMD Fluid Temperatures -- Node 1028 Radial Section

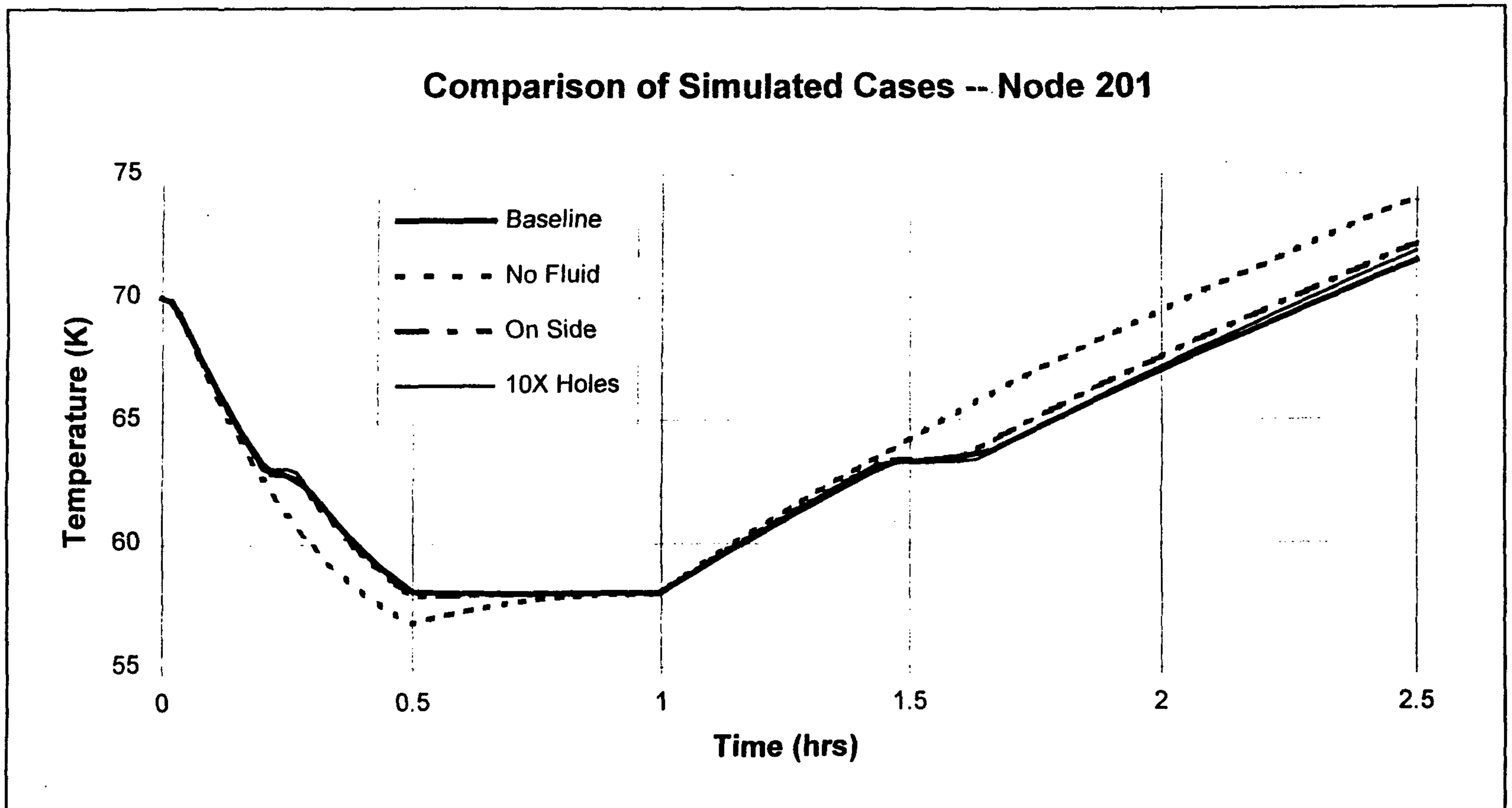

Figure A-8. Comparison of Simulated Cases for Node 201

Appendix B
Listing of SINDA'85 Model

```
HEADER OPTIONS DATA
TITLE      60K SBIR TEST SET-UP
       OUTPUT  =  RGHANSEN.OUT
       QMAP    =  QMAP.OUT
       MODEL   =  TESTPUCK THERMAL MODEL
C
HEADER CONTROL DATA, GLOBAL
C
       ABSZRO  = 0.
       SIGMA   = 5.67E-12
       NLOOPT  = 500
       NLOOPS  = 5000
       TIMEO   = 0.0
       TIMEND  = 3600.*1.
       DTIMEH  = 10.
       OUTPUT  = 60.
       DRLXCA  = .001
       ARLXCA  = .001
       EBALSA  = .001
C
HEADER OPERATIONS DATA
C
DEFMOD     TESTPUCK
BUILD WHOLE,       TESTPUCK
C
C
        F10211=0.
        F10212=0.
        F10213=0.
        F10214=0.
        F10215=0.
        F10216=0.
        F10217=0.
        F10218=0.
C
        F10221=0.
        F10222=0.
        F10223=0.
        F10224=0.
        F10225=0.
        F10226=0.
        F10227=0.
        F10228=0.
C
        F10231=0.
        F10232=0.
        F10233=0.
        F10234=0.
        F10235=0.
        F10236=0.
        F10237=0.
        F10238=0.
C
        F10241=0.
        F10242=0.
        F10243=0.
        F10244=0.
        F10245=0.
        F10246=0.
        F10247=0.
        F10248=0.
C
        F10251=0.
        F10252=0.
        F10253=0.
        F10254=0.
        F10255=0.
        F10256=0.
        F10257=0.
```

```
        F10258=0.
C
        F10261=0.
        F10262=0.
        F10263=0.
        F10264=0.
        F10265=0.
        F10266=0.
        F10267=0.
        F10268=0.
C
        F10271=0.
        F10272=0.
        F10273=0.
        F10274=0.
        F10275=0.
        F10276=0.
        F10277=0.
        F10278=0.
C
        F10281=0.
        F10282=0.
        F10283=0.
        F10284=0.
        F10285=0.
        F10286=0.
        F10287=0.
        F10288=0.
C
        CALL FWDBCK
        CALL QMAP('TESTPUCK',1)
C
HEADER USER DATA, GLOBAL
C
        TMELT=63.15
INCLUDE I1021.FOR
INCLUDE I1022.FOR
INCLUDE I1023.FOR
INCLUDE I1024.FOR
INCLUDE I1025.FOR
INCLUDE I1026.FOR
INCLUDE I1027.FOR
INCLUDE I1028.FOR
C
HEADER USER DATA,       TESTPUCK
C
HEADER ARRAY DATA,      TESTPUCK
C
C...ALUMINUM CONSTANT CP
      1=0.,900.,400.,900.
C
C...ALUMINUM VARIABLE CP
      2=  0.,.001, 50.,142., 60.,214., 70.,287., 80.,357., 90.,422.
        100.,481.,120.,580.,140.,654.,160.,713.,180.,760.,200.,797.
        220.,826.,240.,849.,260.,869.,280.,886.,300.,902.,350.,920.
C
C...ALUMINUM CONSTANT K
      3=0.,210.,400.,210.
C
C...2219 ALUMINUM VARIABLE K
      4=  0.,.001,33.,26.,66.,50.,100.,68.,150.,87.,200.,102.
        250.,114.,300.,123.,350.,130.
C
C...6061-T6 ALUMINUM VARIABLE K
      5=  0.,.001,33.,45.,50.,62.,66.,76.,100.,97.,200.,133.
          250.,144.,300.,154.,350.,161.
C
C...COPPER VARIABLE CP
C
      8=0.,.001,30.,27.,40.,60.,50.,99.,60.,137.,80.,205.,160.,332.
        260.,376.,300.,386.,350.,386.
C
C...NITROGEN CONSTANT CP
      10=0.,1645.,350.,1645.
C
C...NITROGEN CONSTANT K
```

```
     11=0.,.13, 350.,.13
C
HEADER NODE DATA, TESTPUCK
C
C...PUCK EXTERNAL NODES
C
       SIV 201, 53.01 ,A2, .0698      $ PUCK TOP CENTER
       SIV 202, 53.01 ,A2, .1439      $ PUCK TOP EDGE
       SIV 203, 53.01 ,A2, .2773      $ PUCK SIDE UPPER
       SIV 204, 53.01 ,A2, .1545      $ PUCK SIDE LOWER
       SIV 205, 53.01 ,A2, .1036      $ PUCK BOT EDGE
       SIV 206, 53.01 ,A2, .0534      $ PUCK BOT CENTER
C
C...PUCK INTERNAL NODES
C
C......SOLID
C........TOP (T=.8")
       SIV 1001, 53.01 ,A2,0.017026       $ INT REG/TOP ROW/CELL 1
       SIV 1002, 53.01 ,A2,0.014759       $ INT REG/TOP ROW/CELL 2
       SIV 1003, 53.01 ,A2,0.012492       $ INT REG/TOP ROW/CELL 3
       SIV 1004, 53.01 ,A2,0.010224       $ INT REG/TOP ROW/CELL 4
       SIV 1005, 53.01 ,A2,0.007957       $ INT REG/TOP ROW/CELL 5
       SIV 1006, 53.01 ,A2,0.005690       $ INT REG/TOP ROW/CELL 6
       SIV 1007, 53.01 ,A2,0.003423       $ INT REG/TOP ROW/CELL 7
       SIV 1008, 53.01 ,A2,0.001111       $ INT REG/TOP ROW/CELL 8
C
C........MID (T=.8")
       SIV 1011, 53.01 ,A2,0.017026       $ INT REG/MID ROW/CELL 1
       SIV 1012, 53.01 ,A2,0.014759       $ INT REG/MID ROW/CELL 2
       SIV 1013, 53.01 ,A2,0.012492       $ INT REG/MID ROW/CELL 3
       SIV 1014, 53.01 ,A2,0.010224       $ INT REG/MID ROW/CELL 4
       SIV 1015, 53.01 ,A2,0.007957       $ INT REG/MID ROW/CELL 5
       SIV 1016, 53.01 ,A2,0.005690       $ INT REG/MID ROW/CELL 6
       SIV 1017, 53.01 ,A2,0.003423       $ INT REG/MID ROW/CELL 7
       SIV 1018, 53.01 ,A2,0.001111       $ INT REG/MID ROW/CELL 8
C
C........BOT (T=.6275")
       SIV 1021, 53.01 ,A2,0.013355       $ INT REG/BOT ROW/CELL 1
       SIV 1022, 53.01 ,A2,0.011576       $ INT REG/BOT ROW/CELL 2
       SIV 1023, 53.01 ,A2,0.009798       $ INT REG/BOT ROW/CELL 3
       SIV 1024, 53.01 ,A2,0.008020       $ INT REG/BOT ROW/CELL 4
       SIV 1025, 53.01 ,A2,0.006242       $ INT REG/BOT ROW/CELL 5
       SIV 1026, 53.01 ,A2,0.004463       $ INT REG/BOT ROW/CELL 6
       SIV 1027, 53.01 ,A2,0.002685       $ INT REG/BOT ROW/CELL 7
       SIV 1028, 53.01 ,A2,0.000872       $ INT REG/BOT ROW/CELL 8
C
C...FLUID
C
C....41 CIRCUMFERENTIAL HOLES
       SIV 10211, 53.01 , A10,1.21E-3  $ FLUID VOL 1/BOT CELL 1
       SIV 10212, 53.01 , A10,1.05E-3  $ FLUID VOL 2/BOT CELL 1
       SIV 10213, 53.01 , A10,8.90E-4  $ FLUID VOL 3/BOT CELL 1
       SIV 10214, 53.01 , A10,7.26E-4  $ FLUID VOL 4/BOT CELL 1
       SIV 10215, 53.01 , A10,5.66E-4  $ FLUID VOL 5/BOT CELL 1
       SIV 10216, 53.01 , A10,4.03E-4  $ FLUID VOL 6/BOT CELL 1
       SIV 10217, 53.01 , A10,2.42E-4  $ FLUID VOL 7/BOT CELL 1
       SIV 10218, 53.01 , A10,8.08E-5  $ FLUID VOL 8/BOT CELL 1
C....36 CIRCUMFERENTIAL HOLES
       SIV 10221, 53.01 , A10,1.06E-3  $ FLUID VOL 1/BOT CELL 2
       SIV 10222, 53.01 , A10,9.22E-4  $ FLUID VOL 2/BOT CELL 2
       SIV 10223, 53.01 , A10,7.81E-4  $ FLUID VOL 3/BOT CELL 2
       SIV 10224, 53.01 , A10,6.37E-4  $ FLUID VOL 4/BOT CELL 2
       SIV 10225, 53.01 , A10,4.97E-4  $ FLUID VOL 5/BOT CELL 2
       SIV 10226, 53.01 , A10,3.54E-4  $ FLUID VOL 6/BOT CELL 2
       SIV 10227, 53.01 , A10,2.13E-4  $ FLUID VOL 7/BOT CELL 2
       SIV 10228, 53.01 , A10,7.09E-5  $ FLUID VOL 8/BOT CELL 2
C....30 CIRCUMFERENTIAL HOLES
       SIV 10231, 53.01 , A10,8.85E-4  $ FLUID VOL 1/BOT CELL 3
       SIV 10232, 53.01 , A10,7.68E-4  $ FLUID VOL 2/BOT CELL 3
       SIV 10233, 53.01 , A10,6.51E-4  $ FLUID VOL 3/BOT CELL 3
       SIV 10234, 53.01 , A10,5.31E-4  $ FLUID VOL 4/BOT CELL 3
       SIV 10235, 53.01 , A10,4.14E-4  $ FLUID VOL 5/BOT CELL 3
       SIV 10236, 53.01 , A10,2.95E-4  $ FLUID VOL 6/BOT CELL 3
       SIV 10237, 53.01 , A10,1.77E-4  $ FLUID VOL 7/BOT CELL 3
       SIV 10238, 53.01 , A10,5.91E-5  $ FLUID VOL 8/BOT CELL 3
C....25 CIRCUMFERENTIAL HOLES
```

```
       SIV 10241, 53.01 , A10,7.38E-4  $ FLUID VOL 1/BOT CELL 4
       SIV 10242, 53.01 , A10,6.40E-4  $ FLUID VOL 2/BOT CELL 4
       SIV 10243, 53.01 , A10,5.43E-4  $ FLUID VOL 3/BOT CELL 4
       SIV 10244, 53.01 , A10,4.43E-4  $ FLUID VOL 4/BOT CELL 4
       SIV 10245, 53.01 , A10,3.45E-4  $ FLUID VOL 5/BOT CELL 4
       SIV 10246, 53.01 , A10,2.46E-4  $ FLUID VOL 6/BOT CELL 4
       SIV 10247, 53.01 , A10,1.48E-4  $ FLUID VOL 7/BOT CELL 4
       SIV 10248, 53.01 , A10,4.93E-5  $ FLUID VOL 8/BOT CELL 4
C....19 CIRCUMFERENTIAL HOLES
       SIV 10251, 53.01 , A10,5.61E-4  $ FLUID VOL 1/BOT CELL 5
       SIV 10252, 53.01 , A10,4.86E-4  $ FLUID VOL 2/BOT CELL 5
       SIV 10253, 53.01 , A10,4.12E-4  $ FLUID VOL 3/BOT CELL 5
       SIV 10254, 53.01 , A10,3.36E-4  $ FLUID VOL 4/BOT CELL 5
       SIV 10255, 53.01 , A10,2.62E-4  $ FLUID VOL 5/BOT CELL 5
       SIV 10256, 53.01 , A10,1.87E-4  $ FLUID VOL 6/BOT CELL 5
       SIV 10257, 53.01 , A10,1.12E-4  $ FLUID VOL 7/BOT CELL 5
       SIV 10258, 53.01 , A10,3.74E-5  $ FLUID VOL 8/BOT CELL 5
C....14 CIRCUMFERENTIAL HOLES
       SIV 10261, 53.01 , A10,4.13E-4  $ FLUID VOL 1/BOT CELL 6
       SIV 10262, 53.01 , A10,3.58E-4  $ FLUID VOL 2/BOT CELL 6
       SIV 10263, 53.01 , A10,3.04E-4  $ FLUID VOL 3/BOT CELL 6
       SIV 10264, 53.01 , A10,2.48E-4  $ FLUID VOL 4/BOT CELL 6
       SIV 10265, 53.01 , A10,1.93E-4  $ FLUID VOL 5/BOT CELL 6
       SIV 10266, 53.01 , A10,1.38E-4  $ FLUID VOL 6/BOT CELL 6
       SIV 10267, 53.01 , A10,8.27E-5  $ FLUID VOL 7/BOT CELL 6
       SIV 10268, 53.01 , A10,2.76E-5  $ FLUID VOL 8/BOT CELL 6
C....8 CIRCUMFERENTIAL HOLES
       SIV 10271, 53.01 , A10,2.36E-4  $ FLUID VOL 1/BOT CELL 7
       SIV 10272, 53.01 , A10,2.05E-4  $ FLUID VOL 2/BOT CELL 7
       SIV 10273, 53.01 , A10,1.74E-4  $ FLUID VOL 3/BOT CELL 7
       SIV 10274, 53.01 , A10,1.42E-4  $ FLUID VOL 4/BOT CELL 7
       SIV 10275, 53.01 , A10,1.10E-4  $ FLUID VOL 5/BOT CELL 7
       SIV 10276, 53.01 , A10,7.87E-5  $ FLUID VOL 6/BOT CELL 7
       SIV 10277, 53.01 , A10,4.73E-5  $ FLUID VOL 7/BOT CELL 7
       SIV 10278, 53.01 , A10,1.58E-5  $ FLUID VOL 8/BOT CELL 7
C....3 CIRCUMFERENTIAL HOLES
       SIV 10281, 53.01 , A10,8.85E-5  $ FLUID VOL 1/BOT CELL 8
       SIV 10282, 53.01 , A10,7.68E-5  $ FLUID VOL 2/BOT CELL 8
       SIV 10283, 53.01 , A10,6.51E-5  $ FLUID VOL 3/BOT CELL 8
       SIV 10284, 53.01 , A10,5.31E-5  $ FLUID VOL 4/BOT CELL 8
       SIV 10285, 53.01 , A10,4.14E-5  $ FLUID VOL 5/BOT CELL 8
       SIV 10286, 53.01 , A10,2.95E-5  $ FLUID VOL 6/BOT CELL 8
       SIV 10287, 53.01 , A10,1.77E-5  $ FLUID VOL 7/BOT CELL 8
       SIV 10288, 53.01 , A10,5.91E-6  $ FLUID VOL 8/BOT CELL 8
C
C...COLD FINGER
C
       SIV 306, 53.01 ,A2, .0872       $ COLD FINGER TOP FLANGE
       SIV 301, 53.01 ,A2, .00336      $ COLD FINGER NEAR PUCK
       SIV 302, 53.01 ,A2, .00336      $ COLD FINGER 2ND FROM PUCK
       SIV 303, 53.01 ,A2, .00336      $ COLD FINGER MIDDLE
       SIV 304, 53.01 ,A2, .00336      $ COLD FINGER 2ND FROM COOLER
       SIV 305, 53.01 ,A2, .00336      $ COLD FINGER NEAR COOLER
       SIV 307, 53.01 ,A2, .0872       $ COLD FINGER BOT FLANGE
C
C...COLD HEAD
C
       SIV 401, 35.01 ,A8,2.5         $ COLD HEAD
C
C...SHROUD
C
         -901, 297., 1.              $ LN2 SHROUD
C
HEADER SOURCE DATA, TESTPUCK
C
HEADER CONDUCTOR DATA, TESTPUCK
C
C...CONDUCTION
C
C...EXTERNAL-TO-INTERNAL NODES
C
    SIV 1010, 203, 1001, A4,.260  $ PUCK SID UPPER --> TOP ROW CELL 1 (RADIAL)
    SIV 1020, 204, 1011, A4,.260  $ PUCK SID LOWER --> MID ROW CELL 1 (RADIAL)
    SIV 1030, 204, 1021, A4,.201  $ PUCK SID LOWER --> BOT ROW CELL 1 (RADIAL)
    SIV 1040, 206, 1021, A4,.0345 $ PUCK BOT CNTR  --> BOT ROW CELL 1 (AXIAL)
    SIV 1041, 206, 1022, A4,.0299 $ PUCK BOT CNTR  --> BOT ROW CELL 2 (AXIAL)
```

```
     SIV 1042, 206, 1023, A4,.0253 $ PUCK BOT CNTR  --> BOT ROW CELL 3 (AXIAL)
     SIV 1043, 206, 1024, A4,.0207 $ PUCK BOT CNTR  --> BOT ROW CELL 4 (AXIAL)
     SIV 1044, 206, 1025, A4,.0161 $ PUCK BOT CNTR  --> BOT ROW CELL 5 (AXIAL)
     SIV 1045, 206, 1026, A4,.0115 $ PUCK BOT CNTR  --> BOT ROW CELL 6 (AXIAL)
     SIV 1046, 206, 1027, A4,.0069 $ PUCK BOT CNTR  --> BOT ROW CELL 7 (AXIAL)
     SIV 1047, 206, 1028, A4,.0023 $ PUCK BOT CNTR  --> BOT ROW CELL 8 (AXIAL)
C
C...INTERNAL NODE-TO-INTERNAL NODE
C
C.....AXIAL
     SIV 1050, 1001,1011, A4,.0150 $ TOP-TO-MID CELL 1 (AXIAL)
     SIV 1051, 1002,1012, A4,.0130 $ TOP-TO-MID CELL 2 (AXIAL)
     SIV 1052, 1003,1013, A4,.0110 $ TOP-TO-MID CELL 3 (AXIAL)
     SIV 1053, 1004,1014, A4,.0090 $ TOP-TO-MID CELL 4 (AXIAL)
     SIV 1054, 1005,1015, A4,.0070 $ TOP-TO-MID CELL 5 (AXIAL)
     SIV 1055, 1006,1016, A4,.0050 $ TOP-TO-MID CELL 6 (AXIAL)
     SIV 1056, 1007,1017, A4,.0030 $ TOP-TO-MID CELL 7 (AXIAL)
     SIV 1057, 1008,1018, A4,.0010 $ TOP-TO-MID CELL 8 (AXIAL)
C
     SIV 1060, 1011,1021, A4,.0150 $ MID-TO-BOT CELL 1 (AXIAL)
     SIV 1061, 1012,1022, A4,.0130 $ MID-TO-BOT CELL 2 (AXIAL)
     SIV 1062, 1013,1023, A4,.0110 $ MID-TO-BOT CELL 3 (AXIAL)
     SIV 1063, 1014,1024, A4,.0090 $ MID-TO-BOT CELL 4 (AXIAL)
     SIV 1064, 1015,1025, A4,.0070 $ MID-TO-BOT CELL 5 (AXIAL)
     SIV 1065, 1016,1026, A4,.0050 $ MID-TO-BOT CELL 6 (AXIAL)
     SIV 1066, 1017,1027, A4,.0030 $ MID-TO-BOT CELL 7 (AXIAL)
     SIV 1067, 1018,1028, A4,.0010 $ MID-TO-BOT CELL 8 (AXIAL)
C
C.....RADIAL
     SIV 1501, 1001,1002, A4,.1136 $ TOP CELL 1 - TO - TOP CELL 2
     SIV 1502, 1002,1003, A4,.0975 $ TOP CELL 2 - TO - TOP CELL 3
     SIV 1503, 1003,1004, A4,.0805 $ TOP CELL 3 - TO - TOP CELL 4
     SIV 1504, 1004,1005, A4,.0660 $ TOP CELL 4 - TO - TOP CELL 5
     SIV 1505, 1005,1006, A4,.0495 $ TOP CELL 5 - TO - TOP CELL 6
     SIV 1506, 1006,1007, A4,.0339 $ TOP CELL 6 - TO - TOP CELL 7
     SIV 1507, 1007,1008, A4,.0201 $ TOP CELL 7 - TO - TOP CELL 8
C
     SIV 1601, 1011,1012, A4,.1136 $ MID CELL 1 - TO - MID CELL 2
     SIV 1602, 1012,1013, A4,.0975 $ MID CELL 2 - TO - MID CELL 3
     SIV 1603, 1013,1014, A4,.0805 $ MID CELL 3 - TO - MID CELL 4
     SIV 1604, 1014,1015, A4,.0660 $ MID CELL 4 - TO - MID CELL 5
     SIV 1605, 1015,1016, A4,.0495 $ MID CELL 5 - TO - MID CELL 6
     SIV 1606, 1016,1017, A4,.0339 $ MID CELL 6 - TO - MID CELL 7
     SIV 1607, 1017,1018, A4,.0201 $ MID CELL 7 - TO - MID CELL 8
C
     SIV 1701, 1021,1022, A4,.0879 $ BOT CELL 1 - TO - BOT CELL 2
     SIV 1702, 1022,1023, A4,.0755 $ BOT CELL 2 - TO - BOT CELL 3
     SIV 1703, 1023,1024, A4,.0623 $ BOT CELL 3 - TO - BOT CELL 4
     SIV 1704, 1024,1025, A4,.0511 $ BOT CELL 4 - TO - BOT CELL 5
     SIV 1705, 1025,1026, A4,.0383 $ BOT CELL 5 - TO - BOT CELL 6
     SIV 1706, 1026,1027, A4,.0263 $ BOT CELL 6 - TO - BOT CELL 7
     SIV 1707, 1027,1028, A4,.0156 $ BOT CELL 7 - TO - BOT CELL 8
C
C...SOLID-TO-FLUID AND INTRA-FLUID
C
C....41 HOLES
     SIV 3001, 1021,10211,A11,65.9  $ BOT CELL  1-TO-FLUID VOL 1
     SIV 3002,10211,10212,A11,28.8  $ FLUID VOL 1-TO-FLUID VOL 2
     SIV 3003,10212,10213,A11,24.8  $ FLUID VOL 2-TO-FLUID VOL 3
     SIV 3004,10213,10214,A11,20.4  $ FLUID VOL 3-TO-FLUID VOL 4
     SIV 3005,10214,10215,A11,16.8  $ FLUID VOL 4-TO-FLUID VOL 5
     SIV 3006,10215,10216,A11,12.5  $ FLUID VOL 5-TO-FLUID VOL 6
     SIV 3007,10216,10217,A11,8.61  $ FLUID VOL 6-TO-FLUID VOL 7
     SIV 3008,10217,10218,A11,5.13  $ FLUID VOL 7-TO-FLUID VOL 8
C....36 HOLES
     SIV 3011, 1022,10221,A11,57.9  $ BOT CELL  2-TO-FLUID VOL 1
     SIV 3012,10221,10222,A11,25.3  $ FLUID VOL 1-TO-FLUID VOL 2
     SIV 3013,10222,10223,A11,21.7  $ FLUID VOL 2-TO-FLUID VOL 3
     SIV 3014,10223,10224,A11,17.9  $ FLUID VOL 3-TO-FLUID VOL 4
     SIV 3015,10224,10225,A11,14.7  $ FLUID VOL 4-TO-FLUID VOL 5
     SIV 3016,10225,10226,A11,11.0  $ FLUID VOL 5-TO-FLUID VOL 6
     SIV 3017,10226,10227,A11,7.56  $ FLUID VOL 6-TO-FLUID VOL 7
     SIV 3018,10227,10228,A11,4.50  $ FLUID VOL 7-TO-FLUID VOL 8
C....30 HOLES
     SIV 3021, 1023,10231,A11,48.2  $ BOT CELL  3-TO-FLUID VOL 1
     SIV 3022,10231,10232,A11,21.1  $ FLUID VOL 1-TO-FLUID VOL 2
```

```
    SIV 3023,10232,10233,A11,18.1  $ FLUID VOL 2-TO-FLUID VOL 3
    SIV 3024,10233,10234,A11,14.9  $ FLUID VOL 3-TO-FLUID VOL 4
    SIV 3025,10234,10235,A11,12.3  $ FLUID VOL 4-TO-FLUID VOL 5
    SIV 3026,10235,10236,A11,9.18  $ FLUID VOL 5-TO-FLUID VOL 6
    SIV 3027,10236,10237,A11,6.30  $ FLUID VOL 6-TO-FLUID VOL 7
    SIV 3028,10237,10238,A11,3.75  $ FLUID VOL 7-TO-FLUID VOL 8
C....25 HOLES
    SIV 3031, 1024,10241,A11,40.2  $ BOT CELL  4-TO-FLUID VOL 1
    SIV 3032,10241,10242,A11,17.6  $ FLUID VOL 1-TO-FLUID VOL 2
    SIV 3033,10242,10243,A11,15.1  $ FLUID VOL 2-TO-FLUID VOL 3
    SIV 3034,10243,10244,A11,12.5  $ FLUID VOL 3-TO-FLUID VOL 4
    SIV 3035,10244,10245,A11,10.2  $ FLUID VOL 4-TO-FLUID VOL 5
    SIV 3036,10245,10246,A11,7.65  $ FLUID VOL 5-TO-FLUID VOL 6
    SIV 3037,10246,10247,A11,5.25  $ FLUID VOL 6-TO-FLUID VOL 7
    SIV 3038,10247,10248,A11,3.13  $ FLUID VOL 7-TO-FLUID VOL 8
C....19 HOLES
    SIV 3041, 1025,10251,A11,30.5  $ BOT CELL  5-TO-FLUID VOL 1
    SIV 3042,10251,10252,A11,13.4  $ FLUID VOL 1-TO-FLUID VOL 2
    SIV 3043,10252,10253,A11,11.5  $ FLUID VOL 2-TO-FLUID VOL 3
    SIV 3044,10253,10254,A11,9.46  $ FLUID VOL 3-TO-FLUID VOL 4
    SIV 3045,10254,10255,A11,7.77  $ FLUID VOL 4-TO-FLUID VOL 5
    SIV 3046,10255,10256,A11,5.81  $ FLUID VOL 5-TO-FLUID VOL 6
    SIV 3047,10256,10257,A11,3.99  $ FLUID VOL 6-TO-FLUID VOL 7
    SIV 3048,10257,10258,A11,2.38  $ FLUID VOL 7-TO-FLUID VOL 8
C....14 HOLES
    SIV 3051, 1026,10261,A11,22.5  $ BOT CELL  6-TO-FLUID VOL 1
    SIV 3052,10261,10262,A11,9.84  $ FLUID VOL 1-TO-FLUID VOL 2
    SIV 3053,10262,10263,A11,8.46  $ FLUID VOL 2-TO-FLUID VOL 3
    SIV 3054,10263,10264,A11,6.97  $ FLUID VOL 3-TO-FLUID VOL 4
    SIV 3055,10264,10265,A11,5.73  $ FLUID VOL 4-TO-FLUID VOL 5
    SIV 3056,10265,10266,A11,4.28  $ FLUID VOL 5-TO-FLUID VOL 6
    SIV 3057,10266,10267,A11,2.94  $ FLUID VOL 6-TO-FLUID VOL 7
    SIV 3058,10267,10268,A11,1.75  $ FLUID VOL 7-TO-FLUID VOL 8
C....8 HOLES
    SIV 3061, 1027,10271,A11,12.9  $ BOT CELL  7-TO-FLUID VOL 1
    SIV 3062,10271,10272,A11,5.62  $ FLUID VOL 1-TO-FLUID VOL 2
    SIV 3063,10272,10273,A11,4.83  $ FLUID VOL 2-TO-FLUID VOL 3
    SIV 3064,10273,10274,A11,3.98  $ FLUID VOL 3-TO-FLUID VOL 4
    SIV 3065,10274,10275,A11,3.27  $ FLUID VOL 4-TO-FLUID VOL 5
    SIV 3066,10275,10276,A11,2.45  $ FLUID VOL 5-TO-FLUID VOL 6
    SIV 3067,10276,10277,A11,1.68  $ FLUID VOL 6-TO-FLUID VOL 7
    SIV 3068,10277,10278,A11,1.00  $ FLUID VOL 7-TO-FLUID VOL 8
C....3 HOLES
    SIV 3071, 1028,10281,A11,4.82  $ BOT CELL  8-TO-FLUID VOL 1
    SIV 3072,10281,10282,A11,2.11  $ FLUID VOL 1-TO-FLUID VOL 2
    SIV 3073,10282,10283,A11,1.81  $ FLUID VOL 2-TO-FLUID VOL 3
    SIV 3074,10283,10284,A11,1.49  $ FLUID VOL 3-TO-FLUID VOL 4
    SIV 3075,10284,10285,A11,1.23  $ FLUID VOL 4-TO-FLUID VOL 5
    SIV 3076,10285,10286,A11,.918  $ FLUID VOL 5-TO-FLUID VOL 6
    SIV 3077,10286,10287,A11,.630  $ FLUID VOL 6-TO-FLUID VOL 7
    SIV 3078,10287,10288,A11,.375  $ FLUID VOL 7-TO-FLUID VOL 8
C
C...INTRA-PUCK
C
    SIV 2010, 201, 202,A4, .1138  $ PUCK TOP CENTER --> PUCK TOP EDGE
    SIV 2020, 202, 203,A4, .1340  $ PUCK TOP EDGE   --> PUCK SIDE UPPER
    SIV 2030, 203, 204,A4, .0764  $ PUCK SIDE UPPER --> PUCK SIDE LOWER
    SIV 2040, 204, 205,A4, .1078  $ PUCK SIDE LOWER --> PUCK BOT EDGE
    SIV 2050, 205, 206,A4, .1164  $ PUCK BOT EDGE   --> PUCK BOT CENTER
C
C...PUCK-TO-COLD FINGER
C
    SIV 3010, 206, 306,A4, .2253  $ PUCK BOT CENTER --> COLD FINGER TOP FLANGE
C
C...INTRA-COLD FINGER
C
    SIV 3020, 306, 301,A5, .0106  $ CLD FINGER TOP FLNG --> CLD FINGER TOP
    SIV 3030, 301, 302,A5, .0053  $ CLD FINGER TOP      --> CLD FGR 2ND TO TOP
    SIV 3040, 302, 303,A5, .0053  $ CLD FGR 2ND TO TOP  --> CLD FGR 3RD TO TOP
    SIV 3050, 303, 304,A5, .0053  $ CLD FGR 3RD TO TOP  --> CLD FGR 4TH TO TOP
    SIV 3060, 304, 305,A5, .0053  $ CLD FGR 4TH TO TOP  --> CLD FGR 5TH TO TOP
    SIV 3070, 305, 307,A5, .0106  $ CLD FGR 5TH TO TOP  --> CLD FGR BOT FLNG
C
C...COLD FINGER-TO-COOLER
C
    SIV 3080, 307, 401,A4, .2253  $ CLD FGR BOT FLNG --> COOLER INTERFACE
```

```
C
C...RADIATION TO WALLS (CM2)
C
CINCLUDE RAD.SIN
C
HEADER VARIABLES 0,      TESTPUCK
C
HEADER VARIABLES 1,      TESTPUCK
C
C...HEATER ON TOP OF PUCK + PARASITICS
C
      Q201=2.
      Q202=.1
      Q203=.5
      Q204=.5
      Q205=.1
      Q206=.2
C
C     TTEST=ACTUAL TEMPERATURE (K) OF COLD INTERFACE
C     STEST=DESIRED OPERATING TEMPERATURE (K) OF COLD INTERFACE
C
       STEST=50.
       IF (T206.GT.60.) STEST=60.
C
C      IF (T401.LE.50.) STEST=50.
C...COLD FINGER TEMPERATURE CONTROL/SENSOR HEATING SCHEME
C      IF (TIMEN.GT.1.5*3600..AND.TIMEN.LE.5.*3600.) STEST=58.
C      IF (TIMEN.GT.2.*3600.) Q201=1.
C      IF (TIMEN.GT.2.*3600.) STEST=T306
C
      TTEST=T401
      IF (TTEST.LE.300.AND.TTEST.GT.200.)
     1 QTEST=56.0+4.0*(TTEST-200.)/100.
      IF (TTEST.LE.200.AND.TTEST.GT.100.)
     1 QTEST=38.0+18.0*(TTEST-100.)/100.
      IF (TTEST.LE.100.AND.TTEST.GT.050.)
     1 QTEST=16.0+22.0*(TTEST-050.)/050.
      IF (TTEST.LE.050.AND.TTEST.GT.035.)
     1 QTEST= 0.0+16.0*(TTEST-035.)/015.
      Q401=-QTEST
      IF (TTEST.LT.STEST) Q401=Q401
     1                        +MIN(60.,60.*MAX(0.,(STEST-TTEST)/.2))
C
HEADER VARIABLES 2,      TESTPUCK
C
C...MELTING MODEL
C
C..... FTEST = FRACTION LIQUID (-)
C..... ETEST = PHASE CHANGE ENERGY (J)
C..... TTEST = MELTING TEMPERATURE (K)
C..... ZTEST = FRACTION LIQUID AT PREVIOUS TIME STEP (-)
C..... XTEST = SUM OF PHASE CHANGE ENERGY USED
C
C      ETEST=600.
C      TTEST=63.15
C      ZTEST=FTEST
C      IF (T101.LT.TTEST.AND.FTEST.GT.0.)
C     1 FTEST=MIN(1.,MAX(0.,FTEST-C101*(TTEST-T101)/ETEST))
C      IF (T101.GT.TTEST.AND.FTEST.LT.1.)
C     1 FTEST=MIN(1.,MAX(0.,FTEST-C101*(TTEST-T101)/ETEST))
C      IF (FTEST.LT.1..AND.FTEST.GT.0.) XTEST=XTEST+C101*(TTEST-T101)
C      IF (ZTEST.NE.FTEST) T101=TTEST
C
INCLUDE M1021.FOR
INCLUDE M1022.FOR
INCLUDE M1023.FOR
INCLUDE M1024.FOR
INCLUDE M1025.FOR
INCLUDE M1026.FOR
INCLUDE M1027.FOR
INCLUDE M1028.FOR
C
HEADER OUTPUT CALLS,     TESTPUCK
        TIMEN=TIMEN/60.
        TIMEM=TIMEM/60.
        CALL TPRINT ('TESTPUCK')
```

```
C         CALL QPRINT ('TESTPUCK')
        TIMEN=TIMEN*60.
        TIMEM=TIMEM*60.
END OF DATA
```

Appendix C
Listing of Melt Model FORTRAN Code

FILE: M1021.FOR
(additional melt model files M1022.FOR, M1023.FOR,..., M1028.FOR not shown)

```
C
C...MELTING MODEL
C
C..... F# = FRACTION LIQUID (-)
C..... E# = PHASE CHANGE ENERGY (J)
C..... TMELT = MELTING TEMPERATURE (K)
C..... Z# = FRACTION LIQUID AT PREVIOUS TIME STEP (-)
C..... X# = SUM OF PHASE CHANGE ENERGY USED
C
      TMELT=63.15
C
C...CELL 1021
C......NODE 10211
      E10211=140.*.2344
      Z10211=F10211
      IF (T10211.LT.TMELT.AND.F10211.GT.0.)
     1 F10211=MIN(1.,MAX(0.,F10211-C10211*(TMELT-T10211)/E10211))
      IF (T10211.GT.TMELT.AND.F10211.LT.1.)
     1 F10211=MIN(1.,MAX(0.,F10211-C10211*(TMELT-T10211)/E10211))
      IF (F10211.LT.1..AND.F10211.GT.0.)
     1 X10211=X10211+C10211*(TMELT-T10211)
      IF (Z10211.NE.F10211) T10211=TMELT
C......NODE 10212
      E10212=140.*.2031
      Z10212=F10212
      IF (T10212.LT.TMELT.AND.F10212.GT.0.)
     1 F10212=MIN(1.,MAX(0.,F10212-C10212*(TMELT-T10212)/E10212))
      IF (T10212.GT.TMELT.AND.F10212.LT.1.)
     1 F10212=MIN(1.,MAX(0.,F10212-C10212*(TMELT-T10212)/E10212))
      IF (F10212.LT.1..AND.F10212.GT.0.)
     1 X10212=X10212+C10212*(TMELT-T10212)
      IF (Z10212.NE.F10212) T10212=TMELT
C......NODE 10213
      E10213=140.*.1719
      Z10213=F10213
      IF (T10213.LT.TMELT.AND.F10213.GT.0.)
     1 F10213=MIN(1.,MAX(0.,F10213-C10213*(TMELT-T10213)/E10213))
      IF (T10213.GT.TMELT.AND.F10213.LT.1.)
     1 F10213=MIN(1.,MAX(0.,F10213-C10213*(TMELT-T10213)/E10213))
      IF (F10213.LT.1..AND.F10213.GT.0.)
     1 X10213=X10213+C10213*(TMELT-T10213)
      IF (Z10213.NE.F10213) T10213=TMELT
C......NODE 10214
      E10214=140.*.1406
      Z10214=F10214
      IF (T10214.LT.TMELT.AND.F10214.GT.0.)
     1 F10214=MIN(1.,MAX(0.,F10214-C10214*(TMELT-T10214)/E10214))
      IF (T10214.GT.TMELT.AND.F10214.LT.1.)
     1 F10214=MIN(1.,MAX(0.,F10214-C10214*(TMELT-T10214)/E10214))
      IF (F10214.LT.1..AND.F10214.GT.0.)
     1 X10214=X10214+C10214*(TMELT-T10214)
      IF (Z10214.NE.F10214) T10214=TMELT
C......NODE 10215
      E10215=140.*.1094
      Z10215=F10215
      IF (T10215.LT.TMELT.AND.F10215.GT.0.)
     1 F10215=MIN(1.,MAX(0.,F10215-C10215*(TMELT-T10215)/E10215))
      IF (T10215.GT.TMELT.AND.F10215.LT.1.)
     1 F10215=MIN(1.,MAX(0.,F10215-C10215*(TMELT-T10215)/E10215))
      IF (F10215.LT.1..AND.F10215.GT.0.)
     1 X10215=X10215+C10215*(TMELT-T10215)
      IF (Z10215.NE.F10215) T10215=TMELT
C......NODE 10216
      E10216=140.*.0781
      Z10216=F10216
      IF (T10216.LT.TMELT.AND.F10216.GT.0.)
```

```
      1 F10216=MIN(1.,MAX(0.,F10216-C10216*(TMELT-T10216)/E10216))
       IF (T10216.GT.TMELT.AND.F10216.LT.1.)
      1 F10216=MIN(1.,MAX(0.,F10216-C10216*(TMELT-T10216)/E10216))
       IF (F10216.LT.1..AND.F10216.GT.0.)
      1 X10216=X10216+C10216*(TMELT-T10216)
       IF (Z10216.NE.F10216) T10216=TMELT
C......NODE 10217
       E10217=140.*.0469
       Z10217=F10217
       IF (T10217.LT.TMELT.AND.F10217.GT.0.)
      1 F10217=MIN(1.,MAX(0.,F10217-C10217*(TMELT-T10217)/E10217))
       IF (T10217.GT.TMELT.AND.F10217.LT.1.)
      1 F10217=MIN(1.,MAX(0.,F10217-C10217*(TMELT-T10217)/E10217))
       IF (F10217.LT.1..AND.F10217.GT.0.)
      1 X10217=X10217+C10217*(TMELT-T10217)
       IF (Z10217.NE.F10217) T10217=TMELT
C......NODE 10218
       E10218=140.*.0156
       Z10218=F10218
       IF (T10218.LT.TMELT.AND.F10218.GT.0.)
      1 F10218=MIN(1.,MAX(0.,F10218-C10218*(TMELT-T10218)/E10218))
       IF (T10218.GT.TMELT.AND.F10218.LT.1.)
      1 F10218=MIN(1.,MAX(0.,F10218-C10218*(TMELT-T10218)/E10218))
       IF (F10218.LT.1..AND.F10218.GT.0.)
      1 X10218=X10218+C10218*(TMELT-T10218)
       IF (Z10218.NE.F10218) T10218=TMELT
```

DISTRIBUTION LIST

AUL/LSE Bldg 1405 - 600 Chennault Circle Maxwell AFB, AL 36112-6424	1 cy
DTIC/OCP 8725 John J. Kingman Rd, Suite 0944 Ft Belvoir, VA 22060-6218	2 cys
AFSAA/SAI 1580 Air Force Pentagon Washington, DC 20330-1580	1 cy
PL/SUL Kirtland AFB, NM 87117-5776	2 cys
PL/HO Kirtland AFB, NM 87117-5776	1 cy
Official Record Copy PL/VTP/Lt Mike Rich Kirtland AFB, NM 87117-5776	2 cys
PL/VT Dr Wick Kirtland AFB, NM 87117-5776	1 cy